การสังเคราะห์อนุภาคนาโนแคลเซียมคาร์บอเนตซึ่งมีคุณสมบัติไม่ชอบน้ำ
โดยใช้กรดสเตียริกเป็นตัวปรับปรุงพื้นผิว

นางสาวศุภสิตา ยิ่งยง

SYNTHESIS OF HYDROPHOBIC CaCO$_3$ NANOPARTICLES
USING STEARIC ACID AS SURFACE MODIFIER

Miss Supasita Yingyong

A Thesis Submitted in Partial Fulfillment of the Requirements
for the Degree of Master of Engineering Program in Chemical Engineering
Department of Chemical Engineering
Faculty of Engineering
Chulalongkorn University
Academic Year 2012

Thesis Title   SYNTHESIS OF HYDROPHOBIC CaCO$_3$

NANOPARTICLES USING STEARIC ACID AS

SURFACE MODIFIER

By   Miss Supasita Yingyong

Field of Study   Chemical Engineering

Thesis Advisor   Associate Professor Tawatchai Charinpanitkul, D.Eng.

Accepted by the Faculty of Engineering, Chulalongkorn University in Partial Fulfillment of the Requirements for the Master's Degree

.... Dean of the Faculty of Engineering

(Associate Professor Boonsom Lerdhirunwong, Dr.Ing.)

THESIS COMMITTEE

.... Chairman

(Assistant Professor Apinan Soottitantawat, D.Eng.)

.... Thesis Advisor

(Associate Professor Tawatchai Charinpanitkul, D.Eng.)

.... Examiner

(Assistant Professor Varong Pavarajarn, Ph.D.)

.... External Examiner

(Chantamanee Poonjarernsilp, D.Eng.)

ศุภสิตา ยิ่งยง : การสังเคราะห์อนุภาคนาโนแคลเซียมคาร์บอเนตซึ่งมีคุณสมบัติไม่ชอบน้ำโดยใช้กรด
สเตียริกเป็นเป็นตัวปรับปรุงพื้นผิว (SYNTHESIS OF HYDROPHOBIC CaCO$_3$
NANOPARTICLES USING STEARIC ACID AS SURFACE MODIFIER)
อ. ที่ปรึกษาวิทยานิพนธ์หลัก: รศ. ดร. ธวัชชัย ชรินพาณิชกุล, 75 หน้า.

การสังเคราะห์อนุภาคแคลเซียมคาร์บอเนต (CaCO$_3$) ซึ่งมีคุณสมบัติไม่ชอบน้ำสามารถ
เกิดขึ้นได้ด้วยวิธีอย่างง่ายโดยดำเนินการผ่านปฏิกิริยาในตัวกลางที่เป็นน้ำร่วมกับกรดสเตียริก
สารละลายแอมโมเนี่ยมสเตียเรต (C$_{17}$H$_{35}$COONH$_4$) ซึ่งเตรียมได้จากกรดสเตียริกและสารละลาย
แอมโมเนียมไฮดรอกไซด์ (NH$_4$OH) ถูกใช้เป็นสารตั้งต้นสำหรับการปรับปรุงคุณสมบัติพื้นผิวของ
อนุภาคแคลเซียมคาร์บอเนตที่สังเคราะห์ได้ ซึ่งผลที่ได้นั้น ไม่เพียงแต่ควบคุมการเกิดนิวเคลียสและ
การเติบโตของอนุภาคแคลเซียมคาร์บอเนต แต่ยังมีผลต่อการเกิดเป็นสมบัติที่ไม่ชอบน้ำที่ผิวของ
อนุภาคแคลเซียมคาร์บอเนตอีกด้วย ความเข้มข้นเริ่มต้นของสารละลายแคลเซียมไฮดรอกไซด์ที่
เหมาะสมที่สุดที่ทำให้อนุภาคแคลเซียมคาร์บอเนตที่สังเคราะห์ได้มีขนาดและรูปร่างสม่ำเสมอ คือ
2 มิลลิโมลาร์ คิดเป็นร้อยละผลได้เท่ากับ 49 อุณหภูมิในการเกิดปฏิกิริยาคาร์บอเนชันเป็นปัจจัยที่
ส่งผลให้เกิดสัณฐานอราโกไนต์ สัณฐานอราโกไนต์ซึ่งมีรูปร่างคล้ายเข็มถูกสังเคราะห์ได้ที่อุณหภูมิ
60 และ 90 องศาเซลเซียส อย่างไรก็ตาม พบว่าอุณหภูมิที่ใช้ในการบ่มมีอิทธิพลเพียงเล็กน้อยต่อการ
ตกตะกอนอนุภาคแคลเซียมคาร์บอเนต นอกจากนี้ลักษณะทางสัณฐานวิทยา ลักษณะความเป็นผลึก
และหมู่ฟังก์ชันบนพื้นผิวของอนุภาคแคลเซียมคาร์บอเนตจะถูกตรวจสอบลักษณะสมบัติด้วย
เทคนิคกล้องจุลทรรศน์อิเล็กตรอนแบบส่องกราด เทคนิคเอกซเรย์ดิฟแฟรกชันสเปกโตรสโกปี
เทคนิคฟูเรียร์ทรานสฟอร์ม และอินฟาเรดสเปกโตรสโกปี โปรแกรมจัดการทางภาพถูกใช้เพื่อ
ศึกษาความเชื่อมโยงของคุณลักษณะเฉพาะทางกายภาพของอนุภาคกับสภาวะที่ใช้ในการสังเคราะห์
จากผลการทดลอง สามารถสรุปได้ว่าการใช้กรดสเตียริกที่มีการควบคุมอุณหภูมิคาร์โบเนชันเป็น
สิ่งสำคัญในการสังเคราะห์แคลเซียมคาร์บอเนตระดับนาโนที่มีสมบัติไม่ชอบน้ำ

ภาควิชา........วิศวกรรมเคมี.......ลายมือชื่อนิสิต...
สาขาวิชา........วิศวกรรมเคมี.......ลายมือชื่อ อ.ที่ปรึกษาวิทยานิพนธ์หลัก....................................
ปีการศึกษา.........2555.............

5270526921: MAJOR CHEMICAL ENGINEERING
KEYWORDS: CALCIUM CARBONATE / HYDROPHOBIC / CARBONATION / STEARIC ACID

SUPASITA YINGYONG: SYNTHESIS OF HYDROPHOBIC CaCO$_3$ NANOPARTICLES USING STEARIC ACID AS SURFACE MODIFIER. ADVISOR: ASSOC. PROF. TAWATCHAI CHARINPANITKUL, D.Eng., 75 pp.

Facile synthesis of hydrophobic calcium carbonate (CaCO$_3$) had been conducted via aqueous reaction route incorporated with stearic acid. Ammonium stearate (C$_{17}$H$_{35}$COONH$_4$) solution prepared from stearic acid (C$_{17}$H$_{35}$COOH) and ammonium hydroxide (NH$_4$OH) was used as substrate for modifying surface property of the synthesized CaCO$_3$, resulting in not only the nucleation and growth of CaCO$_3$ particles but also formation of hydrophobic surface of CaCO$_3$. The optimal initial calcium hydroxide Ca(OH)$_2$ concentration which provided unique particles size and morphology was 2 mM with 49% yield. The carbonation temperature was an important factorto regulate the formation of aragonite morphology. Needle-like aragonite was precipitated at 60 and 90 °C. However, the incubation temperature was a minor influence for precipitated CaCO$_3$ particles. In addition, morphology, crystallinity and functional groups on surface of CaCO$_3$ were characterized by scanning electron microscopy, X-ray diffraction spectroscopy and Fourier Transform Infrared spectroscopy. Image processing program was employed for examining linkages of particle physical characteristics and the synthesizing conditions. As a result, it could be implied that usage of stearic acid with control of carbonation temperature would be essential for synthesizing nano-scalled CaCO3 with hydrophobic property.

Department: __Chemical Engineering__ Student's Signature…………………….....
Field of Study: __Chemical Engineering__ Advisor's Signature…………………..……
Academic Year: _____2012_____

ACKNOWLEDGEMENTS

CONTENTS

LIST OF TABLES

LIST OF FIGURES

Page

CHAPTER I

INTRODUCTION

1.1 Motivation

Biomineralization is the major natural process invading with for synthesis of inorganic crystals by organic substrate [1]. Calcium carbonate ($CaCO_3$) is the one of the most abundant minerals which is not only building block of some natural materials such as bones and teeth. In addition, $CaCO_3$ is useful filler incorporated in various composite materials such as paper, plastics, paint and rubber [2]. Precipitated calcium carbonate (PCC) is considered to be non-toxic additive. FDA (Food and Drug Administration) has affirmed precipitated calcium carbonate as GRAS (Generally Recognized As Safe). PCC can be used as direct food additive, pharmaceutical additive, or as an indirect additive in paper products that contact with the food. This approval also exists around the world [3].

In general filler must be well dispersed in a polymer matrix. Normal $CaCO_3$ particles possess polarity and hydrophilic property, leading to its agglomeration and incompatibility to non-polar hydrophobic matrix. The technique that can improve the different of polarity is by modifying the surface with hydrophobic species. Biomineralization has inspired for using organic substance as a surfactant which be expected not only be a surface modifier but also control the nucleation and growth of particles [4].

Application of $CaCO_3$ particles depends on various factors, such as morphology, structure, size, chemical purity, brightness, and so on. Among these factors size of and morphology would be recognized as the most interesting factors. It is recognized that precipitated calcium carbonate nanoparticles are high surface area, high reflect index and light scattering coefficient. They could be filled into litho inks for serve as the main rheological additive and cost-reducing filler. In lightly filled offset inks, they are used as thickeners instead of more expensive thickeners and also replace oils and varnishes. The aragonite polymorph exhibits needle-like shape which has the ratio of length-to-diameter of the crystals is called aspect ratio. In the

application of paper coating, high aspect ratio of aragonite tends to high gloss finishes and is better at covering substrates at lower coating thicknesses. Using of high aspect ratio aragonite as additive also can improve strength or impact resistance in polymeric material. In addition, rhombohedral calcite is the most common polymorph and the most stable phase. The rhombohedral and prismatic forms can improve the strength of polymer matrixes in paper application. In filled papers, large prismatic morphologies are useful for improving drainage on the paper machine and providing a bulky finished product. When applied in pigmented size applications, large prismatic PCC can help lower gloss or sheen of the paper surface.

Chen et al synthesized the hydrophobic $CaCO_3$ particles by stearic acid with a high molar ratio of NaOH/stearic acid (ratios: 0.5-2) affected the surface hydrophobicity. The results show the decreasing of contact angle at higher molar ratio. They conclude and suggest the results were relative to electrostatic force which slightly increases the number of negative electricity around stearic acid molecule. The interaction of stearic acid with calcium ion was increased by electrostatic attraction and the hydrophobicity was increased. With the further increase of NaOH, electrostatic repulsion between stearic acid molecules became stronger thus some molecule of stearic acid cannot modify the $CaCO_3$ surface cause the weak hydrophobic surface. The results from this research, we expect to synthesize hydrophobic $CaCO_3$ particles without impurity of sodium ion[5].

In this thesis, synthesis of hydrophobic $CaCO_3$ will be conducted in an aqueous solution incorporated with chemical reaction, so-called "wet chemistry process". The carbonation method is an industrially useful method for wet chemistry process but it is difficult to control the crystal size and shape of $CaCO_3$ particles. Conventionally, surface modification of $CaCO_3$ for excellent surface properties can be realized, but the synthesis of $CaCO_3$ with a modifier is complex process so it requires more complicated treatment. The preparation of organic solution and synthesis of hydrophobic $CaCO_3$ particles could be using the carbonation process would be experimentally examined. The surface modifier will be added into $Ca(OH)_2$ solution before carbonation process. While $CaCO_3$ particles were synthesized in the process of carbonation, surface of $CaCO_3$ particles could also be modified at the same time.

1.2. Objectives

To synthesize hydrophobic $CaCO_3$ nanoparticles using stearic acid as surface modifier.

| Stearic acid 0.001 M | + | NH_4OH 0.001 M |

⬇

| Ammonium stearate | + | $Ca(OH)_2$ |

⬇

Incubation

⬇

| Calcium stearate |

⬇

Carbonation

⬇

Wash, Filter and Dry

⬇
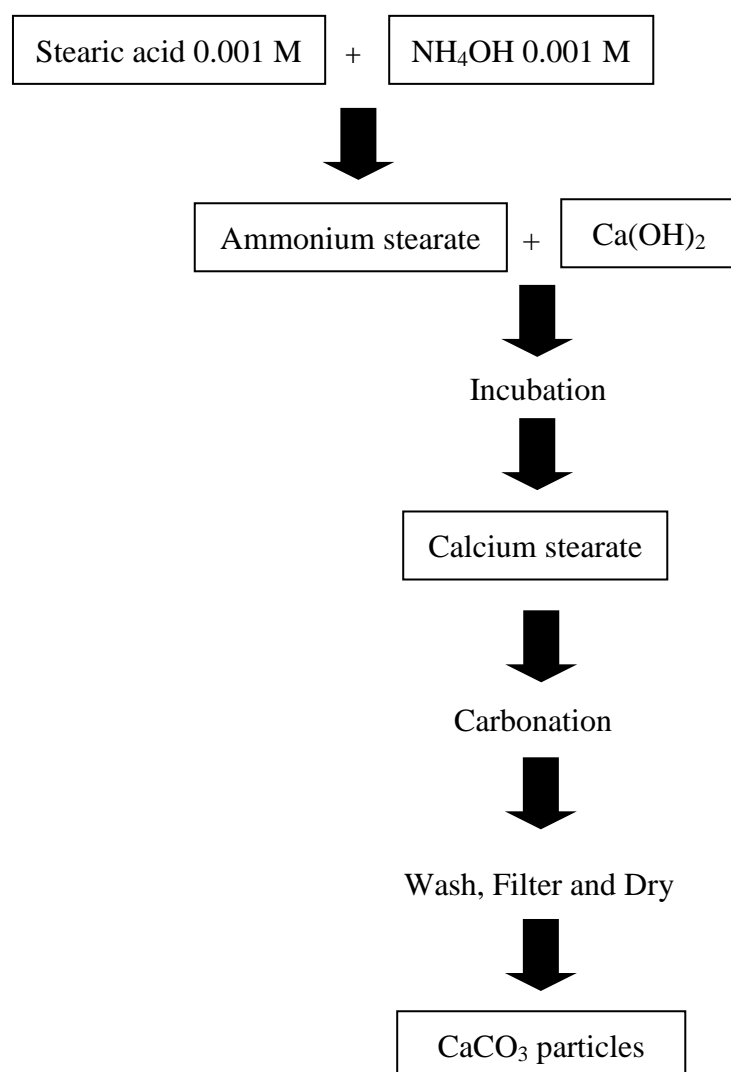
| $CaCO_3$ particles |

Figure 1.1 Methodology for synthesis of hydrophobic $CaCO_3$ nanoparticles

1.3 Scopes

1. Investigation of the influence of preparation parameters on the organic substrates:

1.1 Initial $Ca(OH)_2$ concentration in a range of 1, 2, 3 and 4 mM

1.2 Incubation temperature in a range of 30, 60 and 90 ºC

2. Investigation of the influence of synthesis parameters on the carbonation process:

2.1 Carbonation temperature in a range of 30, 60 and 90 ºC.

2.2 Flow rate of gas mixture (CO_2 and N_2) in a range of 0.1 and 0.2

L/min

3. Characterize precipitated $CaCO_3$ particles:

3.1 Analysis of the surface morphology by scanning electron

microscope (SEM)

3.2 Element analysis by using energy dispersive X-ray spectroscopy

(EDS) (as an integrated feature of SEM)

3.3 Analysis of the $CaCO_3$ crystalline phase by X-ray diffraction XRD)

3.4 Analysis of functional groups for $CaCO_3$ crystalline surface by

Fourier Transform Infrared spectrometer (FT-IR)

3.5 Analysis of zeta potential by zatasizer

3.6 Analysis of the hydrophobic property by using the contact angle

measurement

1.4 Procedure

In this work, Procedure of the thesis was divided into 9 steps as follow;

1. Conduct literature survey and review

2. Prepare of experimental materials and setting up equipment

3. Conduct experiments of preparation of organic solution

4. Characterize precipitated $CaCO_3$ propertied by SEM, XRD, FT-IR

   and contact angle

5. Make discussion on the influence of preparation parameters and

   determination of optimal conditions for using stearic acid as a

   modifier

6. Conduct experiments of synthesis of hydrophobic $CaCO_3$

   nanoparticles

7. Characterize precipitated $CaCO_3$ propertied by SEM, XRD, FT-IR

   and contact angle

8. Prepare conclusion of the experimental results

9. Write thesis and prepare draft manuscript for journal publication

1.5 Expected benefits

To understand the synthesis of $CaCO_3$ particles with modifier on carbonation process for obtain controlled characteristic of $CaCO_3$ particles for $CaCO_3$ nanoparticles.

CHAPTER II

FOUNDAMENTAL KNOWLEDGE AND LITERATURE REVIEWS

2.1 Fundamental Knowledge

This section focuses on the fundamental properties of calcium carbonate, surface modifier and carbonation, including their properties, precipitated method and fields of application.

2.1.1 Calcium carbonate [6]

Calcium carbonate ($CaCO_3$) is an inorganic compound. $CaCO_3$ is non-toxic powder usually white or colorless crystalline compound, occurring naturally as limestone, chalk and marble in all part of the world. $CaCO_3$ is an abundant mineral comprising approximate 4 % of the earth's crust. The component of $CaCO_3$ has three elements which are of particular importance for all organic and inorganic material on our planet (carbon, oxygen and calcium). Calcium carbonate is the active ingredient in agricultural lime, and is usually the principal cause of hard water. It is commonly used medicinally as a calcium supplement or as an antacid, but excessive consumption can be hazardous.

The vast majority of calcium carbonate used in industry is extracted by mining or quarrying. Pure calcium carbonate (e.g. for food or pharmaceutical use), can be produced from a pure quarried source (usually marble).

Figure 2.1 $CaCO_3$ powder

Alternatively, calcium carbonate is prepared from calcium oxide. Water is added to give calcium hydroxide, and carbon dioxide is passed through this solution to precipitate the desired calcium carbonate, referred to in the industry as precipitated calcium carbonate (PCC) [7]:

$$CaCO_3 \rightarrow CaO + CO_2$$

$$CaO + H_2O \rightarrow Ca(OH)_2$$

$$Ca(OH)_2 + CO_2 \rightarrow CaCO_3 + H_2O$$
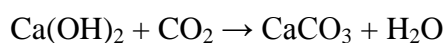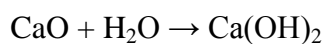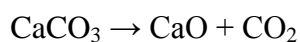
The main use of calcium carbonate is in the construction industry, either as a building material or limestone aggregate for road building or as an ingredient of cement or as the starting material for the preparation of builder's lime by burning in a kiln. However, due to weathering mainly caused by acid rain, calcium carbonate (in limestone form) is no longer used for building purposes on its own, and only as a raw/primary substance for building materials.

In the oil industry, calcium carbonate is added to drilling fluids as a formation-bridging and filtercake-sealing agent; it is also a weighting material which increases the density of drilling fluids to control the downhole pressure. Calcium carbonate is added to swimming pools, as a pH corrector for maintaining alkalinity and offsetting the acidic properties of the disinfectant agent.

Calcium carbonate is widely used medicinally as an inexpensive dietary calcium supplement or gastric antacid [8]. It may be used as a phosphate binder for the treatment of hyperphosphatemia (primarily in patients with chronic renal failure). It is also used in the pharmaceutical industry as an inert filler for tablets and other pharmaceuticals [9].

$CaCO_3$ minerals are the form of polymorphs which usually has three common crystal structures such as rhombohedral form of calcite, spherical vaterite and orthorhombic aragonite. A polymorph is a mineral with the same chemical formula but different chemical and also different physical properties. The arrangement of the ions in crystalline $CaCO_3$ can be described in terms of separate layers of Ca^{2+} cations and CO_3^{2-} anions. Coordination environments for Ca^{2+} ions (CO_3^{2-}, respectively) in the polymorphs differ from each other, as a result of different properties.

1. Calcite [10]

Calcite (*chalix* the Greek word for lime) is so abundant and widely distribution. Calcite is the most stable phase at room temperature under normal atmospheric condition. In calcite, each single packed Ca layer parallel to the plane is situated between single layers of CO_3^{2-}. Each layer of calcite containing anions oriented in opposite directions so each Ca^{2+} ion is situated in distorted octahedral coordination environment of six CO_3^{2-} anions. The hydrophilic of $CaCO_3$ is the result of incomplete coordination of Ca^{2+} ions and CO_3^{2-} ions at the surface of $CaCO_3$ The molecules of water can interact with the space area of surface then get the particles have **"hydrophilic properties"**. The crystals of calcite can form a thousand different shapes such as prism and pinacoid which are the few names of the more common forms of calcite. The most stable morphology of calcite is rhombohedral which is shown in Figure 2.2. The primary mineral component in cave formations is calcite such as stalactites and stalagmites. The crystal is transparent to translucent.

Figure 2.2 Shape of rhombohedral calcite

Many sea organisms such as corals, algae and diatoms make their shells from carbon dioxide gas by pulling carbon dioxide from the sea water. This is fortuitous for us because carbon dioxide gas has been found to be a greenhouse gas and contributes to the so called "greenhouse gas effect". By pulling CO_2 out of the sea water, CO_2 in the air is more dissolve in the sea water and thus acts as a CO_2 filter for the planet. Calcite and other carbonate minerals are very important minerals in the ocean ecosystems of the world.

2. Aragonite [11]
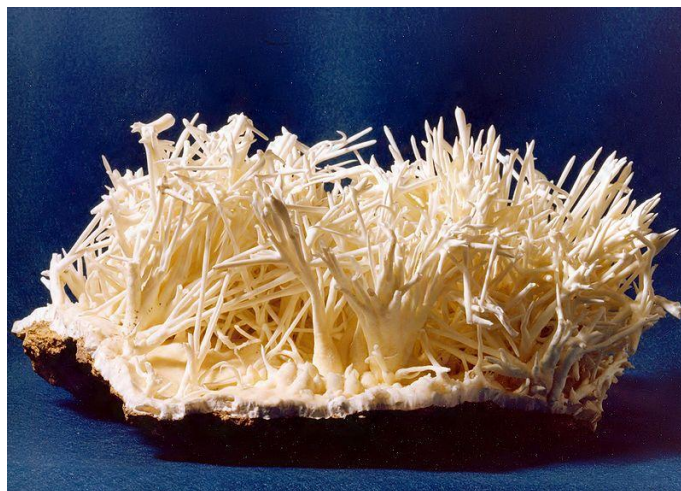
Figure 2.3 Shape of aragonite

Aragonite is one of two common phases of mineral calcium carbonate. Aragonite is formed by biological and physical processes including precipitation from

worm marine and freshwater environments. Aragonite was named followed Aragon region (Spain) where it was found. Aragonite's crystal lattice differs from calcite lattice, resulting in a different crystal shape (orthorhombic). Aragonite may be columnar or fibrous, branching likes flower which is shown in Figure 2.3. Formation of aragonite in the natural is almost all mollusk shells and the calcareous endoskeleton of corals. Because the deposition of mineral in mollusk shells is strongly biologically controlled, some crystal forms are distinctively different from those of inorganic aragonite. The crystal color is white, gray, and yellowish white and sometime colorless. The crystal is transparent to translucent.

3. Vaterite [12]

Figure 2.4 SEM image of the magnified vaterite particles

Vaterite was named after the German chemist and mineralogist Heinrich Vater. The crystal structure is hexagonal this formation is extremely unstable. Vaterite is a metastable phase of calcium carbonate at ambient as less stable than both calcite and aragonite. It is formed at the beginning and then transformed into the more stable calcite (at lower temperature) and aragonite (at higher temperature: about 60 ℃). Vaterite occur in mineral springs, organic tissue, gallstone, and urinary calculi. The physical and optical characteristics of vaterite are similar to calcite. The solubility is better than calcite and aragonite. Vaterite belongs to the hexagonal crystal system and the crystals are always small spherical shape. Figure 2.4 show the SEM image of the magnified vaterite particles.

2.1.2. Stearic acid [13],[14]

Stearic acid which IUPAC systematic name is octadecanoic acid. Its chemical formula is $CH_3(CH_2)_{16}COOH$. A value of k_a is 1.3×10^{-5}. Solubility of stearic acid in water has been reported as about 0.034 g/100 g water (1 mM). Stearic acid is the useful types of saturated fatty acids which are usually come from many animal and vegetable fats and oils. The melting point of stearic acid is 69.6 ℃ and boiling point is 383 ℃. The name comes from the Greek word stéar which means tallow which appears in state of a waxy solid.

Stearic acid is very useful ingredient in making soaps, plastics, oil pastels and cosmetics, and for softening rubber. Stearic acid is used to harden soaps, also used as a parting compound when making plaster castings from plaster piece mold and when making the mold from shellacked clay original. In this use, powdered stearic acid is dissolved in water and the solution. After casting, it is brushed onto the surface to be parted. The term stearate is applied to the salts and esters of stearic acid such as ethylene glycol, glycol stearate and glycol distearate for producing a pearly effect in shampoos, soaps, and other cosmetic products. They add to the product in molten form under controlled conditions for crystallizing. In fireworks, stearic acid is often used to coated-metal powders for preventing oxidation and allowing compositions to be the longer store. It is used along with simple sugar or corn syrup as a hardener in candies.

Stearic acid is used as a surfactant in making soaps. The long chain of carbons and hydrogens ($CH_3(CH_2)_{16}$-) side is a nonpolar hydrocarbon chain that make the soap dissolves in nonpolar materials but not in water. The long chain hydrocarbon is called hydrophobic. The other side of molecule is ionic (the extreme of polarity) so its property likes most ionic compounds. The ionic end of soap could lead to its dissolution in water but not in nonpolar materials. The properties of both hydrophobic and hydrophilic are useful when it comes to cleaning. The hydrophilic end is attracted to the water molecules while the hydrophobic end is attracted to the oily and greasy dirt molecules that repel and come along and wash the dirt away water.

At hard water condition (> 120 mg /L of positively charged Ca^{2+} and Mg^{2+}) the positive Ca^{2+} and Mg^{2+} in the water combine with the negative soap ions and quickly form insoluble salts. These salts are pasty solids that cling to everything. This is the resulting that must to remove the calcium and magnesium ions from the water or replace the soap with something else. Removing the Ca^{2+} and Mg^{2+} is called water softening. The most industrial laundries are done routinely before the water enters the washing equipment by using ion exchange material. This material is replaces the calcium and magnesium ions with sodium ions while the water passes through then the material is kept electrically neutral and positive ion is also located near each negative region. The negative regions are part of the material so they are stationary but the positive ions are mobile [15],[16],[17].

2.1.3 Carbonation [18]

Carbonation is the formation of carbonates which are the salts of carbonic acid (H_2CO_3). Carbon dioxide dissolves in waters to form carbonic acid then carbonic acid dissociates into hydrogen ion and bicarbonate ion. The minerals are attacked with carbonic acid to forming carbonates. Carbonation dominates the weathering of calcareous rock such as limestone and dolomites where the main mineral is calcite or calcium carbonate ($CaCO_3$). Calcite reacts with carbonic acid to form calcium hydrogen carbonate ($Ca(HCO_3)_2$) which readily dissolved in water. The reactions process between carbon dioxide, water, and calcium carbonate may be written.

$$CaCO_3 + H_2O + CO_2 \rightleftharpoons Ca^{2+} + 2HCO_3^-$$
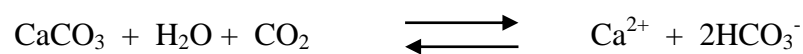
This formula summarizes a sequence that start with dissolve carbon dioxide into water to produce carbonic acid in an ionic state.

$$CO_2 + H_2O \rightleftharpoons H^+ + HCO_3^-$$
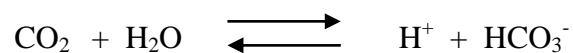
This chemical equilibrium shows that more carbon dioxide and more limestone dissolve into water and react to make more carbonic acid. The process raises the concentration by about 8 mg/L .The carbon dioxide partial pressure from the air (a measure of the amount of carbon dioxide in a unit volume of air) is cause of disequilibrium in water. In response of the chain of reaction, carbon dioxide diffuses

from the air which enables further solution of limestone. The slow process of carbon dioxide diffusion compared with earlier reactions sets the limit for limestone solution rates. Interestingly, the temperature is the cause of the increasing of the reaction rate between carbonic acid and calcite, but the equilibrium solubility of carbon dioxide decreases with temperature. For this reason, high concentrations of carbonic acid may occur in cold regions, even though carbon dioxide is produced at a slow rate by organism in such environments. Carbonation is a step in the complex weathering of many other minerals such as in the hydrolysis of feldspar.

2.1.4 The carbonate system [19]

The relationship between alkalinity and pH is relatively complex. As mentioned in the last section, higher alkalinity tends to prevent water from becoming acidic. In addition, pH influences the type of alkalinity found in water. The **carbonate system**, which is the relationship between pH and the different forms of carbonate - carbonic acid, bicarbonate, and carbonate.
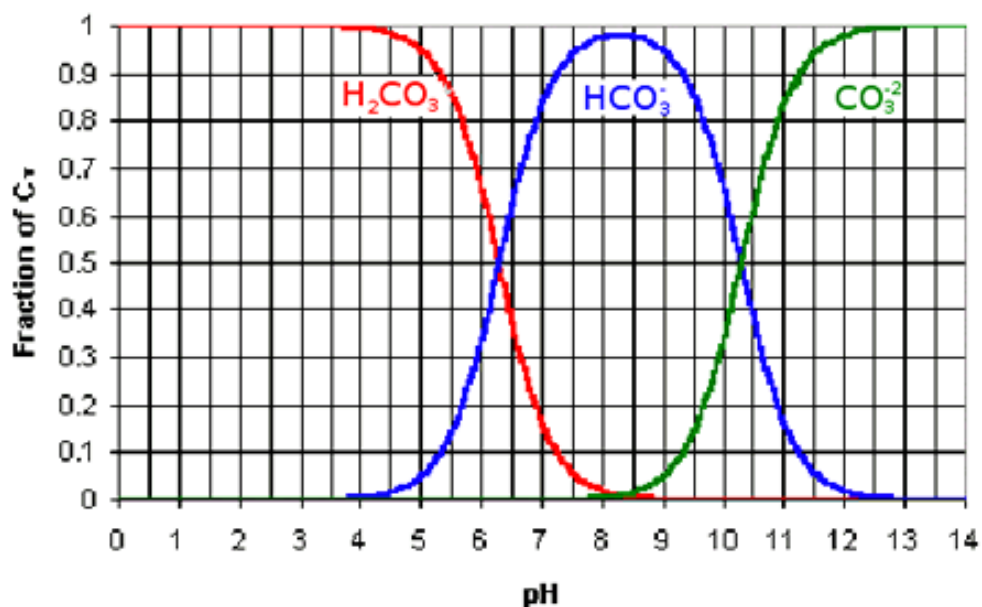
Figure 2.5 Carbonate system

The graph above summarizes the carbonate system. Notice that the form of carbonate in the water is very dependent upon pH. At a low pH, the carbonate is present as carbonic acid. Bicarbonate can be found in water with a pH between 4.3

and 12.3. Above a pH of 8.3, carbonate is also present. Carbon dioxide, carbonic acid, bicarbonate, and carbonate can transform back and forth by gaining or losing hydrogen ions in the reactions shown below:

$$CO_2 + H_2O \longleftrightarrow H_2CO_3$$

$$H_2CO_3 \longleftrightarrow HCO_3^- + H^+$$

$$HCO_3^- \longleftrightarrow CO_3^{2-} + H^+$$
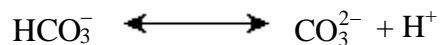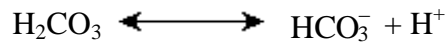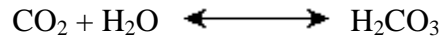
Based on the concentration of hydrogen ions in the solution (the acidity of the solution), various of these reactions will be more or less likely to take place. For example, when the water is very acidic (containing a high concentration of hydrogen ions), the hydrogen ions tend to attach to carbonate or bicarbonate, forming carbonic acid. However, if the water is very basic (containing a lower concentration of hydrogen ions), then carbonic acid tends to break apart, adding hydrogen ions to the solution.
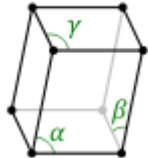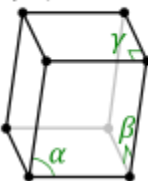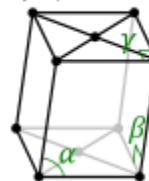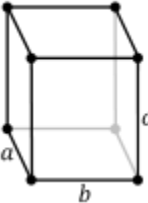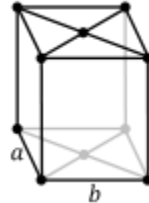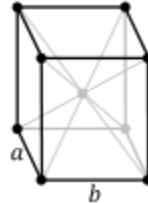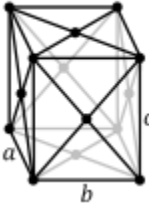
2.1.5 Crystal structure
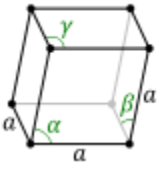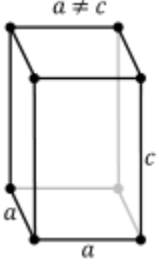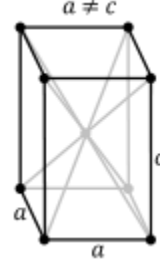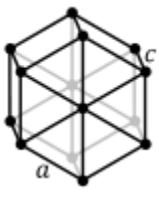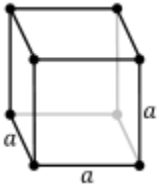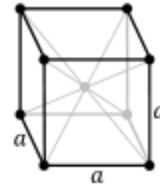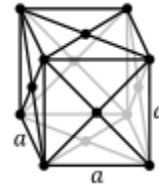
In mineralogy and crystallography, crystal structure is a unique arrangement of atoms or molecules in a crystallineliquid or solid [20]. A crystal structure is composed of a pattern, a set of atoms arranged in a particular way, and a lattice exhibiting long-range order and symmetry. Patterns are located upon the points of a lattice, which is an array of points repeating periodically in three dimensions. The points can be thought of as forming identical tiny boxes, called unit cells, that fill the space of the lattice. The lengths of the edges of a unit cell and the angles between them are called the lattice parameters. The symmetry properties of the crystal are embodied in its space group.

A crystal's structure and symmetry play a role in determining many of its physical properties, such as cleavage, electronic band structure, and optical transparency.

These lattice systems are a grouping of crystal structures according to the axial system used to describe their lattice. Each lattice system consists of a set of three axes in a particular geometrical arrangement. There are seven lattice systems. They are similar to but not quite the same as the seven crystal systems and the six crystal families.

Table 2.1 The 7 lattice systems

The 7 lattice systems (From least to most symmetric)	The 14 Bravais Lattices			
1. triclinic (none)	$\alpha, \beta, \gamma \neq 90°$			
2. monoclinic (1 diad)	simple	base-centered		
	$\alpha \neq 90°$ $\beta, \gamma = 90°$	$\alpha \neq 90°$ $\beta, \gamma = 90°$		
3. orthorhombic (3 perpendicular diads)	simple	base-centered	body-centered	face-centered
	$a \neq b \neq c$	$a \neq b \neq c$	$a \neq b \neq c$	$a \neq b \neq c$

4. rhombohedral (1 triad)	$\alpha=\beta=\gamma \neq 90°$		
5. tetragonal (1 tetrad)	simple	body-centered	
	$a \neq c$	$a \neq c$	
6. hexagonal (1 hexad)			
7. cubic (4 triads)	simple (SC)	body-centered (bcc)	face-centered (fcc)

The simplest and most symmetric, the cubic (or isometric) system, has the symmetry of a cube, that is, it exhibits four threefold rotational axes oriented at 109.5° (the tetrahedral angle) with respect to each other. These threefold axes lie along the body diagonals of the cube. The other six lattice systems, are hexagonal, tetragonal, rhombohedral (often confused with the trigonal crystal system), orthorhombic, monoclinic and triclinic.

2.2 Literature reviews

There have been a number of previous studies on the precipitation process of $CaCO_3$ with the difference purpose in the literature. Some representation works have been surveyed and summarized as follows,

2.2.1 The factors affecting the phase and morphology of PCC

Han et al investigated effect of preparation parameter on the morphology of PCC. They added ammonia into $CaCl_2$ solution then precipitated $CaCO_3$ particles were synthesized from carbonation method. The results showed effect of initial $CaCl_2$ concentration, flow rate and temperature played the important role on phase and morphology of PCC. The particles preferred to form spherical vaterite when the solution has low concentration of $CaCl_2$ (from 0.001 M to 0.1 M) or high flow rate of gas mixture (0.9 L/min to 3 L/min). The needle-like aragonite only be prepared at 60 ºC, this result indicated the temperature is factor for the formation of aragonite [2].

Han et al research effect of flow rate and CO_2 content on the phase and morphology of $CaCO_3$ prepared by bubbling method. They used $CaCl_2$ and CO_2 as the reactant of carbonation reaction. They found that the increase of flow rate over 0.91 L/min, the transformation of calcite to vaterite begins. The increase of CO_2 content from 33.3% to 66.6% is a minor influence because the morphology of samples does not change obviously. Both the results of flow rate and CO_2 content seem to obey the Ostwald's step rules. It indicates that at low supersaturation is influential on the precipitated of stable form which is rhombohedral calcite [21].

2.2.2 The results from adding organic substrates as a modifier to get specific properties of $CaCO_3$ particles

Surface modification of $CaCO_3$ with hydrophobic species, could provide other possible applications. The inorganic mineral particles like $CaCO_3$ are hardly dispersed in polymer matrix. Moreover some of hydrophobic species can also develop the characteristic of particles.

Bei et al attempted to study and control synthesis of cubic $CaCO_3$ particles using polyacrylic acid (PAA) in the aqueous solution. They found that monodispersed cubic calcium carbonate composite particles were prepared by the precipitation reaction of Na_2CO_3 with $CaCl_2$ in water in the presence of polyacrylic acid (PAA) at $60 - 80$ ºC. They also suggested about strong interaction between carboxylic acid group of PAA and calcium ion which influenced the nucleation and growth of $CaCO_3$ particles. The particle size of this research is about 5 microns and some of the particles agglomerated [22].

Sheng et al could to prepare superfine $CaCO_3$ particles using octadecyl dihydrogen phosphate (ODP) as a size-controlling additive and modifier. They also compared the addition of ODP in different reaction periods. The optimal dosage (ratio of ODP to PCC is 1 %) can reduce size of $CaCO_3$ when ODP was added at the digestion period. The addition of ODP in the digestion period could inhibit the crystal growth of $CaCO_3$, while the addition of ODP at pH 7 of the medium could modify surface with hydrophobic property and improve the dispersion of PCC in polyolefinic matrix [23].

Wang et al research a novel aqueous-phase route to synthesize hydrophobic $CaCO_3$ particles in situ. Hydrophobic $CaCO_3$ particles were prepared by carbonation of $Ca(OH)_2$ slurry in the presence of the ethanol solution of oleic acid. The results showed the calcite morphology with ellipse-like shape. The contact angle of modified $CaCO_3$ was 108.77 which showed that $CaCO_3$ particles were very good hydrophobic property [4].

Roberts et al attempted to study phase transitions of adsorbed carboxylic acids on zinc oxide and of zinc soaps by using Infrared data and X-ray diffraction for investigation. Their reaction between carboxylic acids in benzene solution and suspended zinc oxide particles was investigated. The results show the chemisorption of the carboxyl group reacts with the zinc oxide to form zinc carboxylate group. The chemisorption of carboxylic acid forms a multilayer at the surface which gives a new explanation of the protective action of adsorbed acids against flocculation of the particles in nonpolar solvents [24].

2.2.3 The some advantage of surface-modified PCC

Lam et al synthesized precipitated $CaCO_3$ (PCC) nanoparticles and surface-modified PCC nanoparticles. They used carbonation method with crystallization inhibitor (polyphosphate) and surface modifier (stearic acid). They concluded that PCC nanoparticles which were prepared from both of crystallization inhibitor and surface modifier have the highest ability to disperse in polypropylene (PP) matrix. The interaction between PCC interface and PP matrix are better when   15 - 20 wt% of these nanoparticles were added. The yield strength and Young's modulus of PP polymer also increase [25].

Gao et al synthesize and characterize of well-dispersed polyurethane/$CaCO_3$ nanocomposites from a high molecular weight phosphate ester (PPG-P) which was obtained by the reaction of poly (propylene glycol) (PPG1000) with polyphosphoric acid (PPA). The surface treated $CaCO_3$ with PPG-P would disperse well in polyol and nanocomposites because of their good compatibility. The dispersion quality of $CaCO_3$ particles in polyurethane (PU) was greatly improved by the addition of PPG-P. Moreover, the addition of $CaCO_3$ modified by PPG-P improved the thermal property of polyurethane without disrupting the intrinsic structure of PU [26].

Karamipou et al studied the effect of $CaCO_3$ nanoparticles on rheological and dynamic mechanical properties of polypropylene. The $CaCO_3$ nanoparticle content was 5, 10 or 15 wt% with the addition of 1 wt% stearic acid in order to prevent coalescence of nanoparticles were added to the polypropylene by dry mixing before melt extrusion. The $CaCO_3$ nanoparticles were observed to be dispersed uniformly but with a different level of coalescence, especially at high concentration of nanoparticles. At high temperatures, the presence of $CaCO_3$ nanoparticles enables the matrix to sustain a high modulus value [27].

CHAPTER III

RESEARCH METHODOLOGY

The experimental procedures are designed as primary guideline base on the literature survey. The main objective of this thesis is synthesis of hydrophobic $CaCO_3$ nanoparticles. The hydrophobic surface property of $CaCO_3$ nanoparticles have to prepare through organic solution (ammonium stearate).The organic solution will be added into $Ca(OH)_2$ solution before carbonation process. Precipitated $CaCO_3$ particles were synthesized in carbonation process, thus organic substrate will control the growth of particles and also modified surface at the same time.

3.1. Preparation of the organic substrate

In order to prepare organic substrate using as surface modifier, characteristics of the substrate, such as structure and modified ability would be investigated. In this work, preparation conditions of organic substrate would be examined to determine a suitable condition which is the incubation temperature.

3.1.1 Raw materials and equipment

Chemicals and raw materials required for preparation of organic substrate by using stearic acid were shown in Table 3.1.

Table 3.1 Chemicals used for preparation of the organic substrate

Chemical	Formula	Manufacturer	Country
Stearic acid	$C_{17}H_{35}COOH$	Ajax Finechem	Australia
Calcium oxide	CaO	Ajax Finechem	Australia
Ammonium hydroxide	NH_4OH	Mallinckrodt	U.S.A.
De-ionized water	H_2O	Purelab classic DI, ELGA	UK

3.1.2 Experimental

Calcium oxide (CaO) was digested in distilled water to form calcium hydroxide slurry of a certain concentration and kept overnight. The slurry was filtered through a filler paper, liquid part was collect as $Ca(OH)_2$ stock solution.

1 mM of Stearic acid ($C_{17}H_{35}COOH$) was added into 200 ml hot de-ionized water to form suspension. Then, 1 mM of NH_4OH was introduced into suspension. This suspension was stirred vigorously for several minutes to obtain a saponification solution for using as organic substrate. The different concentration of $Ca(OH)_2$ (1, 2, 3 and 4 mM) was added into the organic substrate. The mixture was incubated at different temperatures (30, 60 and 90 °C) in order that Ca^{2+} could associate with the organic substrate to form chemical bond by interface recognition of molecules.

3.2 Synthesis of hydrophobic $CaCO_3$ particles by using carbonation process

In order to synthesize $CaCO_3$ particles via carbonation reaction, characteristics of the products, such as morphology, size, crystal structure, functional group and hydrophobic property would be investigated. In this work, synthesis conditions of $CaCO_3$ particles would be examined to determine a suitable condition, such as initial $Ca(OH)_2$ concentration, carbonation temperature and total CO_2/N_2 flow rate.

3.2.1 Raw materials

In this section, CO_2 gas was bubbled through organic solution in carbonation process for synthesize precipitated $CaCO_3$ particles. Some gases used in this process were listed in Table 3.3.

Table 3.2 Chemicals used for carbonation reaction

Chemical	Formula	Manufacturer	Country
High purity carbon dioxide	CO_2 (g.)	Thai Industrial Gas	Thailand
High purity nitrogen	N_2 (g.)	Thai Industrial Gas	Thailand

3.2.2 Experimental

The procedure for synthesis of $CaCO_3$ is carbonation of the mixture by bubbling CO_2/N_2 gas mixture. CO_2 and N_2 were mixed with volumetric ratio of 1:1 before introducing into the slurry with different total flow rate (0.1 and 0.2 L/min). The reaction was undergone at different carbonation temperatures. $CaCO_3$ crystals are form and grow while pH value of slurry was decreased. The reaction is stopped when the final pH value of suspension is 7. The crystalline $CaCO_3$ particles was rinsed off for remove contaminating of organic substrates and then dried at 110 °C in an oven to obtain the hydrophobic $CaCO_3$ nanoparticles before characterization of the obtained solid sample.

3.3 Analytical instruments

In this thesis work, various analytical instruments were employed to determine physical and chemical properties of precipitated products, such as microstructure, functional group, crystal structure, hydrophobic property, zeta potential and pH value of solution. Some detail and specifications of that analytical instrument were shown below.

3.3.1 Scanning Electron Microscopy (SEM)

Morphology of the precipitated $CaCO_3$ was studied by using scanning electron microscope (SEM; model JSM-6400) equipped with the energy dispersive X-ray spectroscopy (EDS) at Scientific and Technological Research Equipment Centre Foundation, Chulalongkorn University. A photo of the Scanning Electron Microscopy (SEM) machine is shown in Figure 3.1.

Figure 3.1 Scanning Electron Microscope (SEM, model JSM-6400)

3.3.2 X-Ray Diffraction (XRD)

Structure and crystallinity of precipitated $CaCO_3$ at all carbonation temperature were characterized by X-ray diffraction analysis (XRD; Bruker AXS model D8 discover) at Scientific and Technological Research Equipment Centre Foundation, Chulalongkorn University using CuKα radiation, with 40 kV and 40 mA, at 0.02° scan rate (in 2θ) with step of 0.2 s per step. Figure 3.2 shows the XRD analysis system used in this work.

Figure 3.2 X-Ray Diffraction (XRD; Bruker AXS model D8 discover)

3.3.3 Fourier Transform – Infrared Spectroscopy (FT-IR)

Function groups of samples were identified by using Fourier transform infrared spectrophotometer (FT-IR, Thermo Scientific: model Nicolet 6700) located at Center of Excellence in Particle and Technology Engineering laboratory, Chulalongkorn University (shown in Figure 3.3). The infrared spectra were recorded between wavenumber of 400 and 4000 cm^{-1} with 2 cm^{-1} resolution and 100 scanning for the measurement.

Figure 3.3 Fourier Transform Infrared Spectroscopy (FT-IR Thermo Scientific: model Nicolet 6700)

3.3.4 Zetasizer

The surface charge of precipitated CaCO$_3$, pure CaCO$_3$ and stearic acid were characterized by measurement of its zeta potential using a zetasizer (Malvern: model Nano – ZS) (shown in Figure 3.4). This instrument located at National Metal and Materials Technology Center (MTEC).
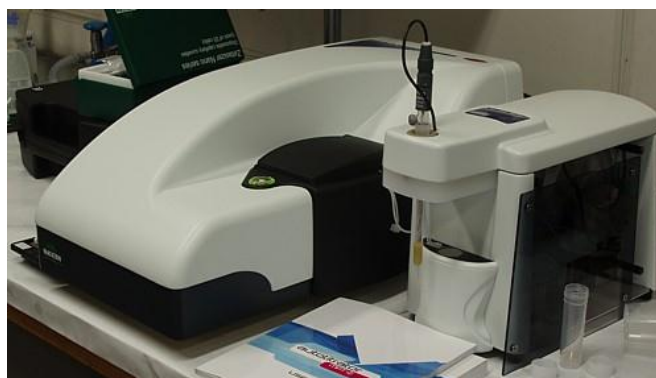
Figure 3.4 Zetasizer (Malvern: model Nano – ZS)

3.3.5 Contact angle

The hydrophobic property of precipitated $CaCO_3$ particles after rinsed off and dried in an oven were measured the contact angle value by using Goniometer (ramé-hart: Model 200-F1). This instrument located at Organic Synthesis Research Unit, Chulalongkorn university.
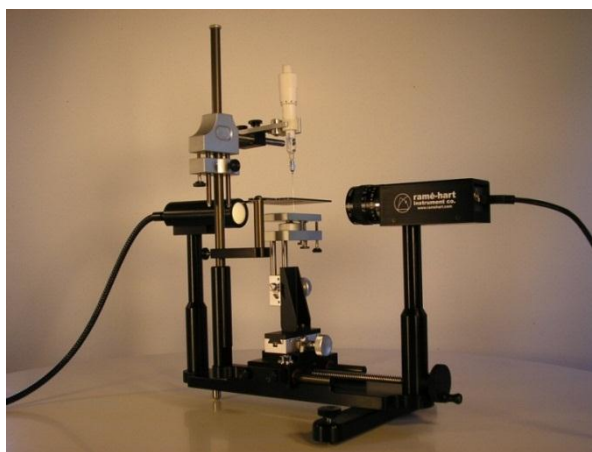
Figure 3.5 Goniometer (ramé-hart: Model 200-F1)

3.3.6 pH Meter

The pH measurements of the solutions after the carbonation reaction were measured by using the pH meter (Mettler Toledo: Five Easy model FE20) (shown in Figure 3.6) which located at Excellence in Particle and Technology Engineering laboratory, Chulalongkorn University.

Figure 3.6 pH meter (Mettler Toledo, Five Easy model FE20)

CHAPTER IV

RESULTS AND DISCUSSION

In this thesis, synthesis of hydrophobic $CaCO_3$ will be conducted in an aqueous solution incorporated with chemical reaction, so-called "wet chemistry process". The carbonation method is an industrially useful method for wet chemistry process but it is difficult to control the crystal size and shape of $CaCO_3$ particles. Conventionally, surface modification of $CaCO_3$ for excellent surface properties can be realized, but the synthesis of $CaCO_3$ with a modifier is complex process so it requires more complicated treatment. The preparation of organic solution and synthesis of hydrophobic $CaCO_3$ particles could be used the carbonation process would be experimentally examined. The surface modifier will be added into $Ca(OH)_2$ solution before carbonation process. While $CaCO_3$ particles were synthesized in the process of carbonation, surface of $CaCO_3$ particles could also be modified at the same time.

There are 4 main scopes of thesis. There are the influence of initial $Ca(OH)_2$ concentration, incubation temperature, carbonation temperature and flow rate of CO_2/N_2. We will study about the size, crystal structure and morphology of precipitated $CaCO_3$.

4.1 Effect of initial $Ca(OH)_2$ concentration

The synthesis of hydrophobic $CaCO_3$ was conducted in an aqueous solution which is incorporated with chemical reaction called carbonation. The preparation of organic solution and synthesis of hydrophobic $CaCO_3$ particles incorporated with carbonation process was experimentally examined. Stearic acid which is the surface modifier was added into $Ca(OH)_2$ solution before carbonation process with an expectation to control size and hydrophobicity of $CaCO_3$ particles.

Figure 4.1 shows the effect of initial $Ca(OH)_2$ concentration on the size and morphology of $CaCO_3$ particles which the stearic acid concentration, the total CO_2/N_2

(1:1, v/v) flow rate, temperature and stirring rate were kept constant at 1 mM, 0.2 L/min, 30 ºC, 400 rpm, respectively. The morphology of $CaCO_3$ particles was sensitive to the variation of initial $Ca(OH)_2$ concentration. $1 - 2$ mM of initial $Ca(OH)_2$ concentration was obtained the uniform small particles. Moreover, rhombohedral calcite particles with small particles were formed with initial $Ca(OH)_2$ concentration of 3 - 4 mM. For the particle size analysis based on image processing, it was found that the synthesized $CaCO_3$ particles exhibit a normal distribution behavior. The small synthesized particles, which were 275±61 nm and 300±41 nm of mean diameter, were obtained from 1 and 2 mM of initial $Ca(OH)_2$ concentration, respectively. With the further increase in the initial $Ca(OH)_2$ concentration to 3 and 4 mM (Figure 4.1c and 4.1d), the mean diameter of small $CaCO_3$ particles were 325±60 and 280±42 nm which was mixed with the large cubic particles. The large cubic particle size was about 3.1 µm.

The precipitated $CaCO_3$ without using stearic acid as a surface modifier was shown in Figure 4.1e. The average diagonal of rhombohedral calcite particles were 5 µm (size = 3.6 µm). The effect of stearic concentration to initial $Ca(OH)_2$ concentration ratio (1:1, 1:2, 1:3 and 1:4 molar ratio) on the precipitated $CaCO_3$ size was shown in Figure 4.1a – 4.1d. 1:1 and 1:2 molar ratio of stearic acid concentration to initial $Ca(OH)_2$ concentration ratio could uniformly control the size of the precipitated $CaCO_3$ particles. However, at 1:3 and 1:4 molar ratio could control only size of some particles. It should be noted that the optimal initial $Ca(OH)_2$ concentration for precipitation of small $CaCO_3$ particles was 2 mM which was 49 % yield of precipitated $CaCO_3$.
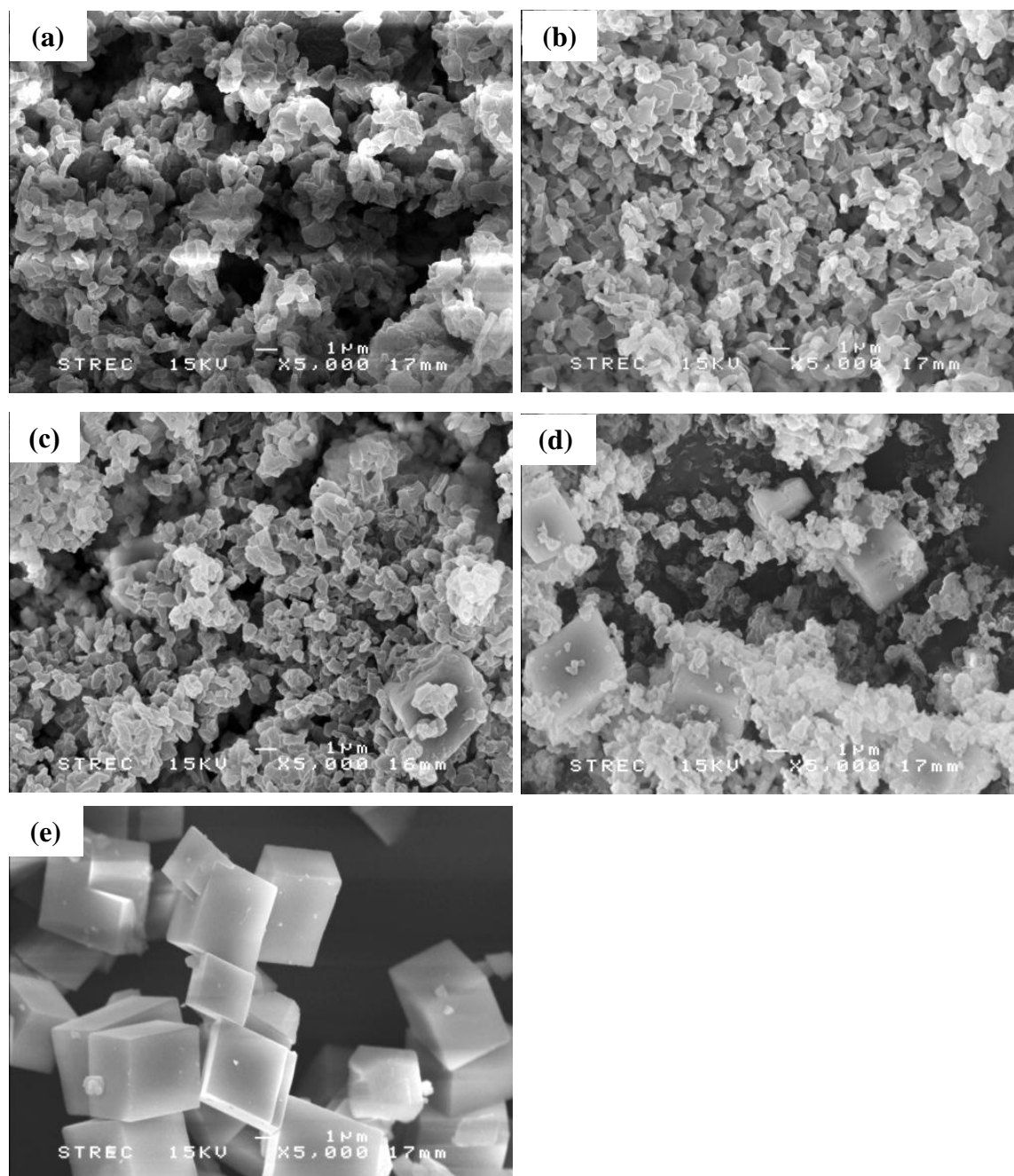
Figure 4.1 Typical SEM images of CaCO$_3$ particles prepared at different initial Ca(OH)$_2$ concentration of (a) 1 mM, (b) 2 mM, (c) 3 mM, (d) 4 mM and (e) Unmodified CaCO$_3$

In the order to comfirm the crystal structure of precipitated $CaCO_3$ particles, X-Ray diffraction was investigated. Comparison of XRD patterns of the precipitated products which was synthesized at constant temperature of 30 ºC with different initial $Ca(OH)_2$ concentration from 1 mM to 4 mM were shown in Figure 4.2. Typical XRD patterns of calcium stearate were detected at 2θ values of 20.3, 21.7, 23.1 and 26.3 deg. Similar XRD pattern revealing the existence of calcium stearate was also reported by Mehmet et al [28].The patterns indicated the calcium stearate which was the bonding at $CaCO_3$ surface.

It should be noted that XRD patterns at 2θ values of 26.2, 29.5, 35.9, 39.5, 43.2, 47.6 and 48.5 deg. were calcite structure of $CaCO_3$ which are ascribed to [102], [104], [110], [113], [202], [024], and [116], respectively [29]. The calcite pattern appear on the entire products from 1 mM to 4. Therefore, it is reasonably implied that the result of XRD pattern could confirm the presence of calcite and calcium stearate in the precipitated $CaCO_3$ particles.

Even though the SEM images of precipitated $CaCO_3$ particles prepared at different initial $Ca(OH)_2$ concentration (Figure 4.1) show the different of size and shape but the results from XRD patterns could confirm the presence of only crystal structure of calcite. So it means that the stearic acid which is using as surface modifier can control the particle size without changing of crystal structure of precipitated $CaCO_3$.
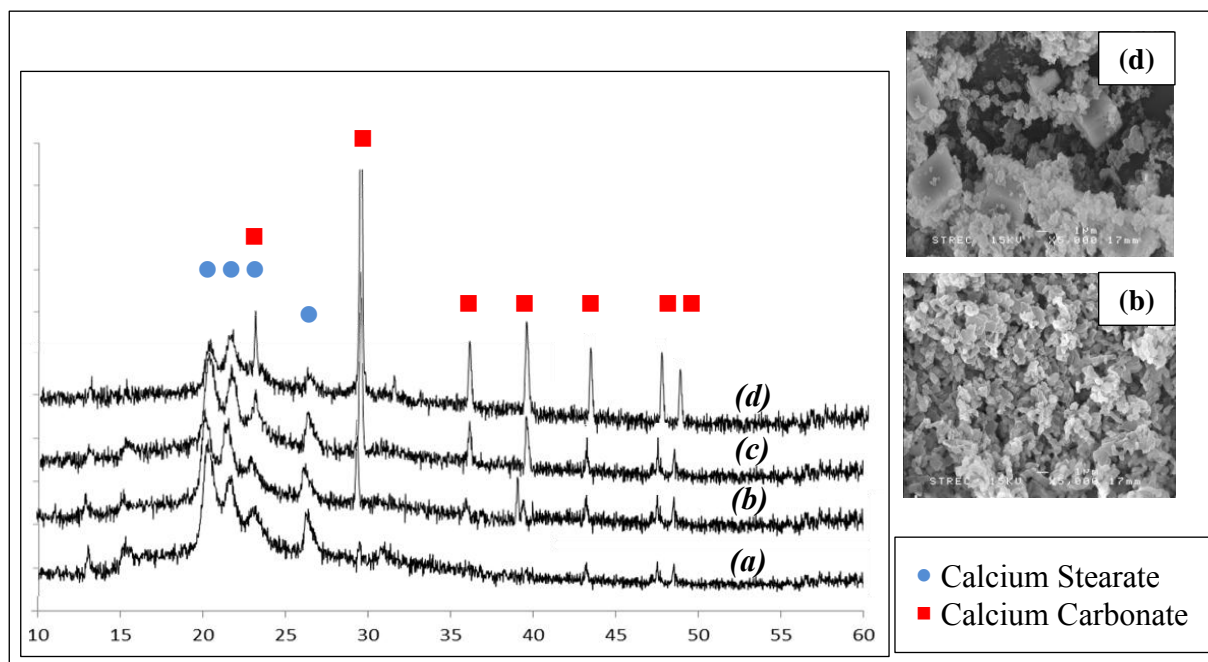
Figure 4.2 X-ray diffraction diagrams of products prepared at different initial CaCO₃ concentration (a) 1mM, (b) 2mM, (c) 3 mM and (d) 4mM

Figure 4.3 shows FT-IR spectra of precipitated $CaCO_3$ at initial $Ca(OH)_2$ concentrations of 2 mM at constant temperature of 30 ºC prepared by KBr in comparison with that of pure $CaCO_3$ particles and pure stearic acid. The free carbonate anions are predicted that there will be three fundamental IR active bands in the spectra [30]. The fundamental bands at 712, 874 and 1420 cm^{-1} are in-plane-bending, out-of-plane bending, and the asymmetric stretching, respectively. The combination bands are also observed at 1797, 2512, and 2917 cm^{-1} [31]. The large vibrational band from 1250 – 1600 cm^{-1} contains the fundamental degenerate stretching frequency of carbonate at 1420 cm^{-1}. For the FTIR spectra of precipitated $CaCO_3$, the strong peak at 1703 cm^{-1} and broad peak around 2800 – 3200 cm^{-1} of pure stearic acid which corresponds to -C=O stretching and O-H stretching of carboxylic acid group was absence. This peak not appears at the precipitated $CaCO_3$ because carboxylic acid group was changed to form carboxylate group. The characteristic bands of stearate group at 1541 and 1561 cm^{-1} can be assigned to the symmetric and asymmetric stretching vibration [32]. The peaks at 1427 and 1468 cm^{-1} are the peak of bending from long chain hydrocarbon. The strong peaks occurred

around 2800 - 3000 cm^{-1} are characteristic of C-H symmetric and asymmetric stretching vibrations, which is the long chain of hydrocarbon from stearic acid, respectively. We could observe the band centered at 1111 cm^{-1} in Figure 4.3 which was assigned to the O–Ca band of $(C_{17}H_{35}COO)_2Ca$. This result indicated that the organic additive was bound onto the surface of precipitated $CaCO_3$ [33],[34],[35],[36].

The stretching of O–Ca band and stretching of carboxylate appear on the precipitated $CaCO_3$, we could conclude the interaction between $CaCO_3$ surface and the surface modifier. Form the previous data, we propose the procedure which is started from CO_2 was added into the saturated Ca^{2+} solution until it saturated with CO_3^{2-} and Ca^{2+}, the consequence will be the form of nucleation. In addition, the particles continue growing and chemisorption at $CaCO_3$ surface which against the agglomeration (See in Figure 4.4). Roberts and Friberg investigated a similar interaction process with zinc xide where several chemisorbed layers of carboxylic group of stearic acid were detected [24].
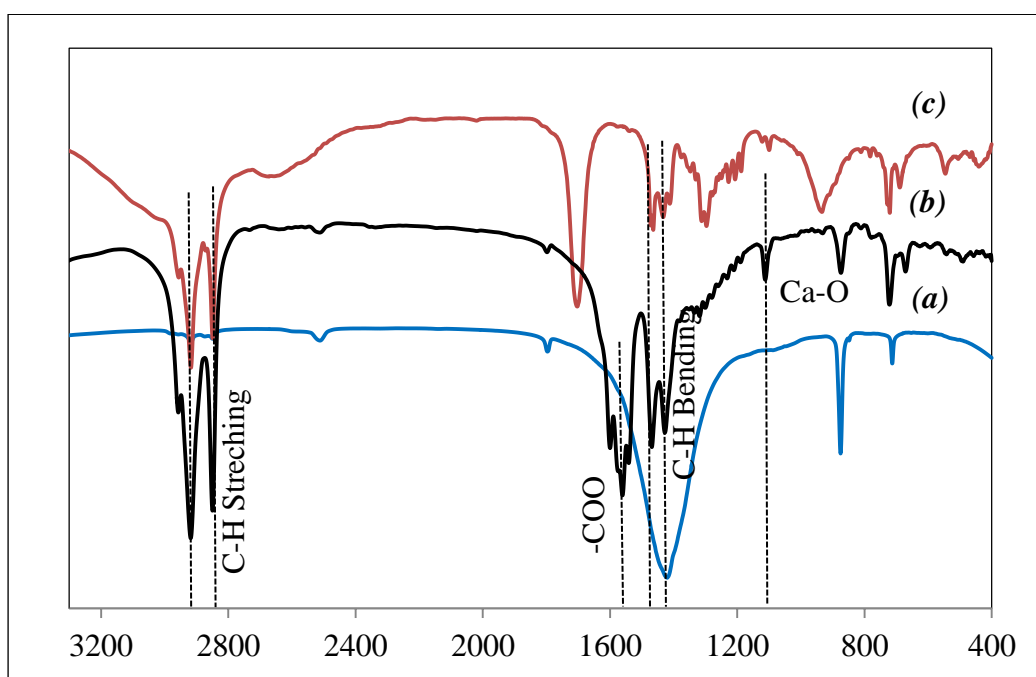
Figure 4.3 FTIR of the b.) precipitated $CaCO_3$ compared with a.) pure $CaCO_3$ and c.) stearic acid
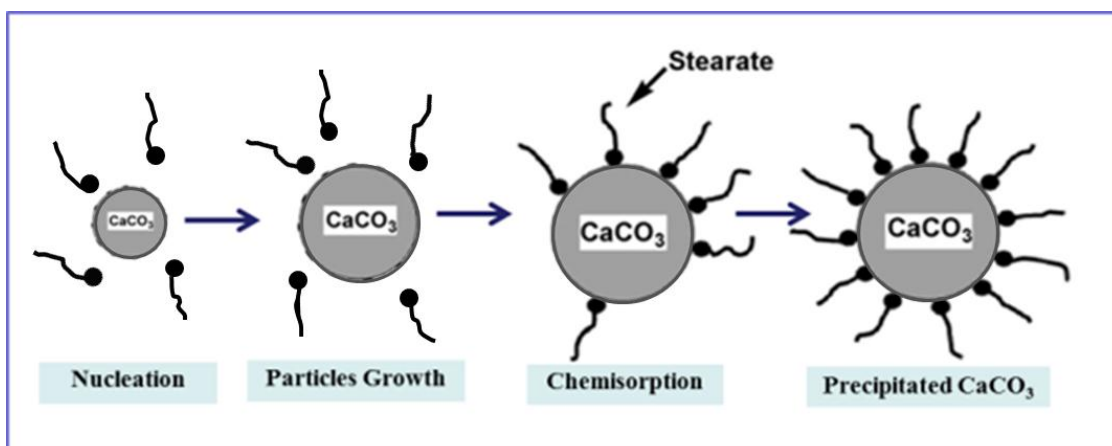
Figure 4.4 Schematic diagram of precipitated $CaCO_3$ by using stearic acid as surface modifier
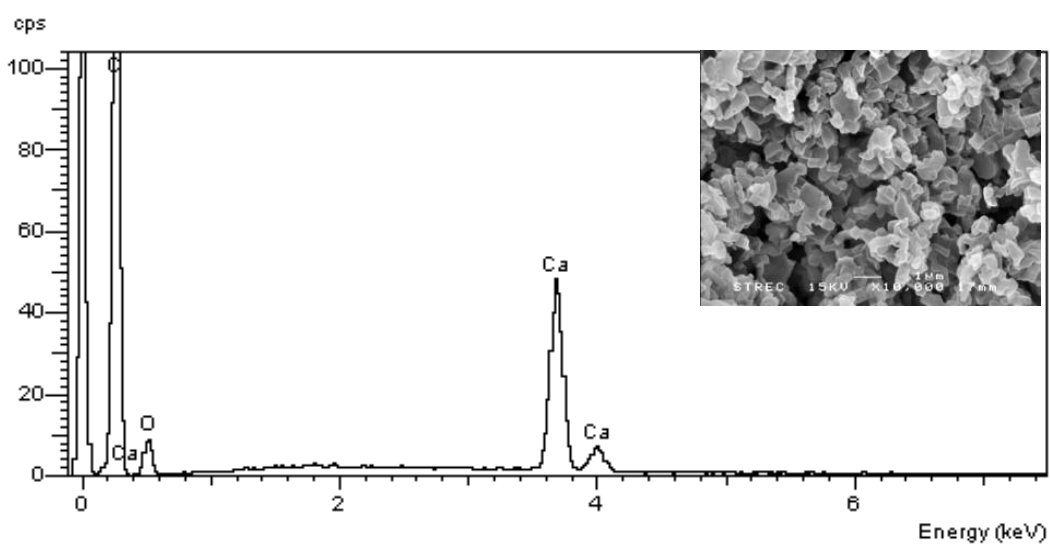
Figure 4.5 Determination of the chemical species present in the precipitated $CaCO_3$ by elemental analysis using energy dispersion spectroscopy (EDS)

Figure 4.5 shows precipitated $CaCO_3$ particles prepared at initial $Ca(OH)_2$ concentrations of 2 mM at constant temperature of 30 ºC were characterized by using elementary analysis (EDS) to confirm the presence of $CaCO_3$ with stearic acid. EDS results show that the sample consisted of C, O, and Ca, the right compositions of $CaCO_3$ and $(C_{17}H_{35}COO)_2Ca$ (calcium stearate). The peak intensity of C was very strong, implying that the quantity of long chain hydrocabon of stearate existed in the products. In addition, elementary analysis (EDS) does not show the impurity peak which is the advantage of this thesis.The only one impurity in this method is NH_4OH which was used for help stearic acid dissolve in water but it was removed since the sample was rinsed off and dried at 110 ºC in an oven.

In order to study the surface characteristics, the precipitated $CaCO_3$ samples were analyzed with measurement of relative contact angle by the sessile drop method. The contact angle was often used to measure the extent of hydrophobic character of solid surfaces. Figure 4.6 shows the sessile drop profiles on the precipitated $CaCO_3$ produced from powders after drying at 110 ºC for 24 h obtained in the absence (pure $CaCO_3$) and presence of surface modifier during in preparation process. It can be seen that when the water droplet was dropped onto the surface of pure $CaCO_3$ powders sample (Figure 4.6a), drop shape was formed. The contact angle of water on pure $CaCO_3$ powders was 111±6 degree. Adding surface modifier which is stearic acid to the process of the preparation of $CaCO_3$, the relative contact angle was increased to 153±2 degree (Figure 4.6b). The increase of contact angle means super hydrophobic property. In the reaction, the surface modifier which is the type of organic substrate had both hydrophilic head and hydrophobic tail. Via the molecular recognition, the hydrophilic head associated with Ca^{2+} and the structure of $(C_{17}H_{35}COO)_2$–$CaCO_3$ was formed, in accordance with $(C_{17}H_{35}COO)_2Ca$ (calcium stearate) covered the $CaCO_3$ surface. Meanwhile, the hydrophobic tail outward changed the surface property of $CaCO_3$ particles, from hydrophilic to hydrophobic.
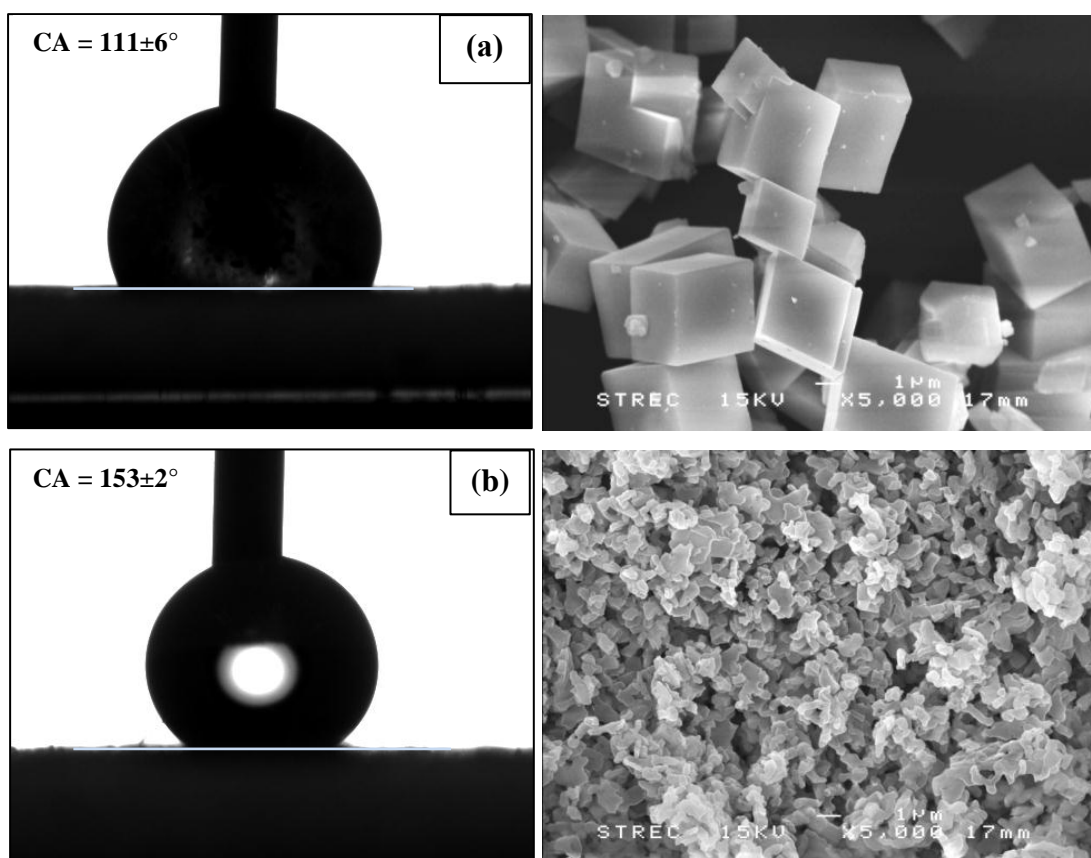
Figure 4.6 Contact angle on calcium carbonate products obtained in (a) absence and (b) presence of surface modifier

Zeta potentials were used to investigate the surface charge of pure $CaCO_3$, stearic acid, precipitated $CaCO_3$ prepared at different carbonation temperature (30, 60 and 90 ºC) are shown in table 4.1. The highest (-15.6 mV) and lowest (-35.4 mV) values were found from pure $CaCO_3$ and stearic acid, respectively, with precipitated $CaCO_3$ at carbonation temperature of 30, 60 and 90 ºC presenting zeta potential values in between (-24.9, -29.8, -33.8 mV). This phenomenon indicates that precipitated $CaCO_3$ at entire carbonation temperature presented an intermediate behavior in terms of surface charge when compared to pure $CaCO_3$ and stearic acid. The decrease of zeta potential of precipitated $CaCO_3$ compared with the pure $CaCO_3$ because it probably the high negative charges of stearic acid which was using as the surface modifier interact with the surface of $CaCO_3$ particles. The results also could be confirmed the chemisorption of $CaCO_3$ surface and stearic acid that tends to increase the surface hydrophobicity which against the agglomeration.

Table 4.1 Zeta potential values of the precipitated $CaCO_3$ products prepared at different carbonation temperature, pure $CaCO_3$ and stearic acid.

Component	Zeta potential (mV)
Pure $CaCO_3$	-15.6
Stearic acid	-35.4
$CaCO_3$ @T=30 ºC	-24.9
$CaCO_3$ @T=60 ºC	-29.8
$CaCO_3$ @T=90 ºC	-33.8

4.2 Effect of incubation temperature

Figure 4.7 shows the effect of incubation temperature from 30, 60 and 90 ºC on the size and shape of $CaCO_3$ particles where the initial $Ca(OH)_2$ concentration, the total CO_2/N_2 flow rate (1:1, v/v), carbonation temperature and stirring rate were kept constant at 2 mM, 0.2 L/min, 30 ºC, 400 rpm, respectively. The $CaCO_3$ particles size was quite changed with the variation of incubation temperature. The small particles without the large rhombohedral particles can precipitated from all these condition. For the particle size analysis based on image processing, it was found that the synthesized $CaCO_3$ exhibits a normal distribution. The precipitated $CaCO_3$ mean diameter of 300±41 nm was obtained when incubated at 30 ºC whereas with further increase in the incubation temperature to 60 and 90 ºC (Figure 4.7b and 4.7c), the mean diameter of $CaCO_3$ particles was quite increased to 380±80 nm and 400±96 nm, respectively. The increasing of incubating temperature tended to increase the particles size, thus the high temperature could be used to destroy activity of the surfactant and also make surfactant unstable [37].

Particles shape and size were quite changed with increase in incubation temperature. In the order to comfirm the crystal structure of precipitated $CaCO_3$ particles, X-Ray diffraction was investigated.
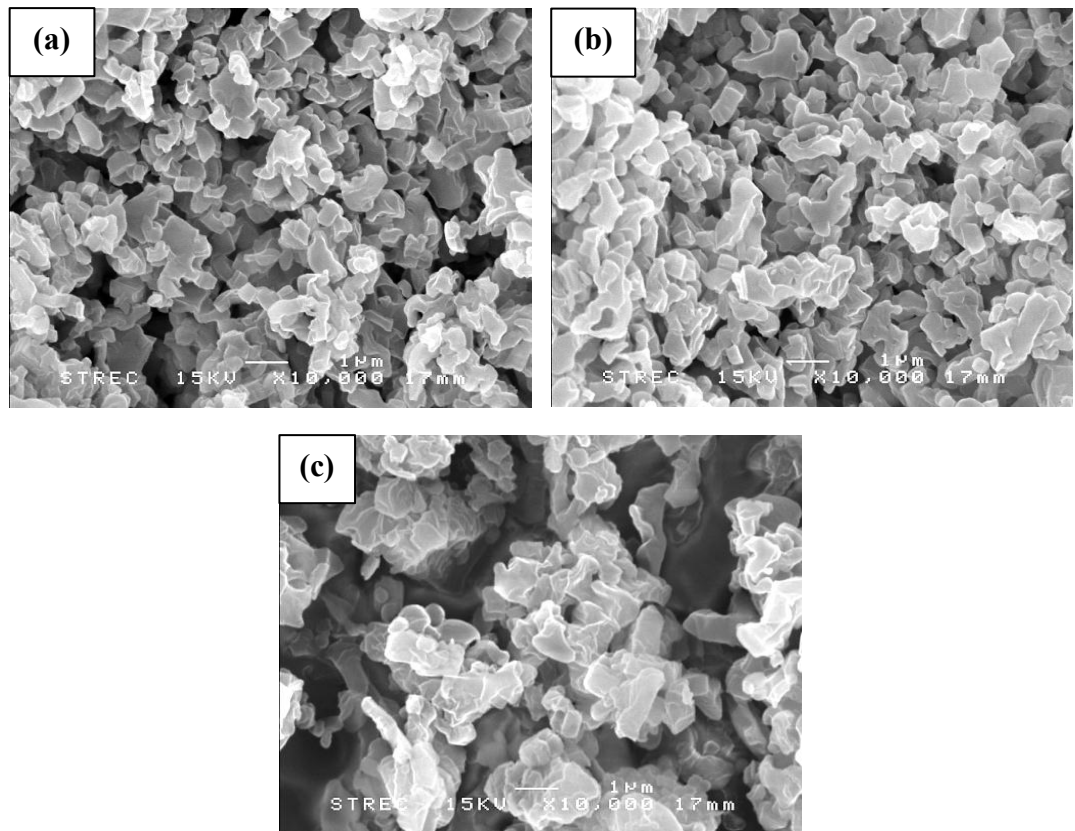
Figure4.7 Typical SEM images of CaCO$_3$ particles prepared at different incubation temperature (a) 30 ℃, (b) 60 ℃ and (c) 90 ℃

Figure 4.2 show the comparison of XRD patterns of the precipitated products which was synthesized at constant initial Ca(OH)$_2$ concentration of 2 mM and constant carbonation temperature of 30 ℃ with different incubation temperature from 30 ℃ to 90 ℃. Typical XRD patterns of calcium stearate were detected at 2θ values of 20.3, 21.7, 23.1 and 26.3 deg. which are shown at all products. Similar XRD pattern revealing the existence of calcium stearate was also reported by Mehmet et al [30].The patterns indicated the calcium stearate which was the bonding at CaCO$_3$ surface.

It should be noted that XRD patterns at 2θ values of 26.2, 29.5, 35.9, 39.5, 43.2, 47.6 and 48.5 deg. were calcite structure of CaCO$_3$ which are ascribed to [102], [104], [110], [113], [202], [024], and [116], respectively [29]. The calcite pattern appear on the entire products from 30 ℃ to 90 ℃ which was no signal for amorphous phase. Therefore, it is reasonably implied that the result of XRD pattern

could confirm the presence of calcite and calcium stearate in the precipitated $CaCO_3$ particles.

Even though the SEM images of precipitated $CaCO_3$ particles prepared at different incubation temperature (Figure 4.7) show the different size and shape but the results from XRD patterns could confirm the presence of only calcite polymorph. So it means that the stearic acid which was using as surface modifier could control the particle size without changing of morphology. The activity of surface modifier decrease with increase incubation temperature, it probably the cause of shape and size change. It should be noted that the proportion of calcium stearate peaks to calcite peaks also decrease with increase in incubation temperature which means the activity of surface modifier decrease.
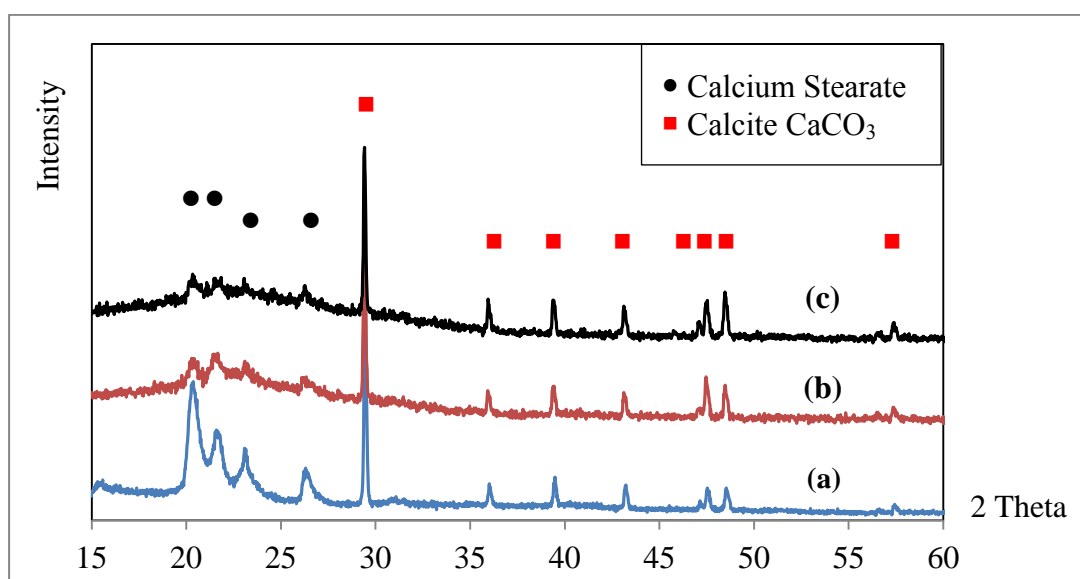
Figure 4.8 X-ray diffraction diagrams of products prepared at different incubation temperature (a) 30 ℃, (b) 60 ℃ and (c) 90 ℃

Figure 4.9 shows FTIR spectra of precipitated $CaCO_3$ at different incubation temperature (30, 60 and 90 ℃) where the initial $Ca(OH)_2$ concentration, carbonation temperature and total CO_2/N_2 (1:1, v/v) flow rate were kept constant at 2 mM, of 30 ℃ and 0.2 L/min . The carbonate fundamental bands of $CaCO_3$ at 712 and 874 cm^{-1} which are in-plane-bending and out-of-plane bending. The combination of carbonate bands are also observed at 1797 and 2512 cm^{-1} [31]. There are characteristic

carboxylate peaks of stearate at 1541 and 1561 cm^{-1} can be assigned to the symmetric and asymmetric stretching vibration of carbonate group [31]. The peaks at 1427 and 1468 cm^{-1} are the peak of C-H bending from long chain hydrocarbon of stearate group. The strong peaks occurred around 2800 - 3000 cm^{-1} are characteristic of C-H symmetric and asymmetric stretching vibrations, which is the long chain of hydrocarbon from stearate, respectively. For all precipitated CaCO$_3$ prepared at defferent incubation temperature, we could conclude that the band centered at 1111 cm^{-1} in Figure 4.9 is assigned to the O–Ca band of (C$_{17}$H$_{35}$COO)$_2$Ca. This results indicate that the organic additive was bound onto the surface of precipitated CaCO$_3$ [33],[34],[35],[36]. After compaing FTIR analysis, all precipitated CaCO$_3$ from incubation temperature of 30, 60 and 90 ℃ had the same functional group.
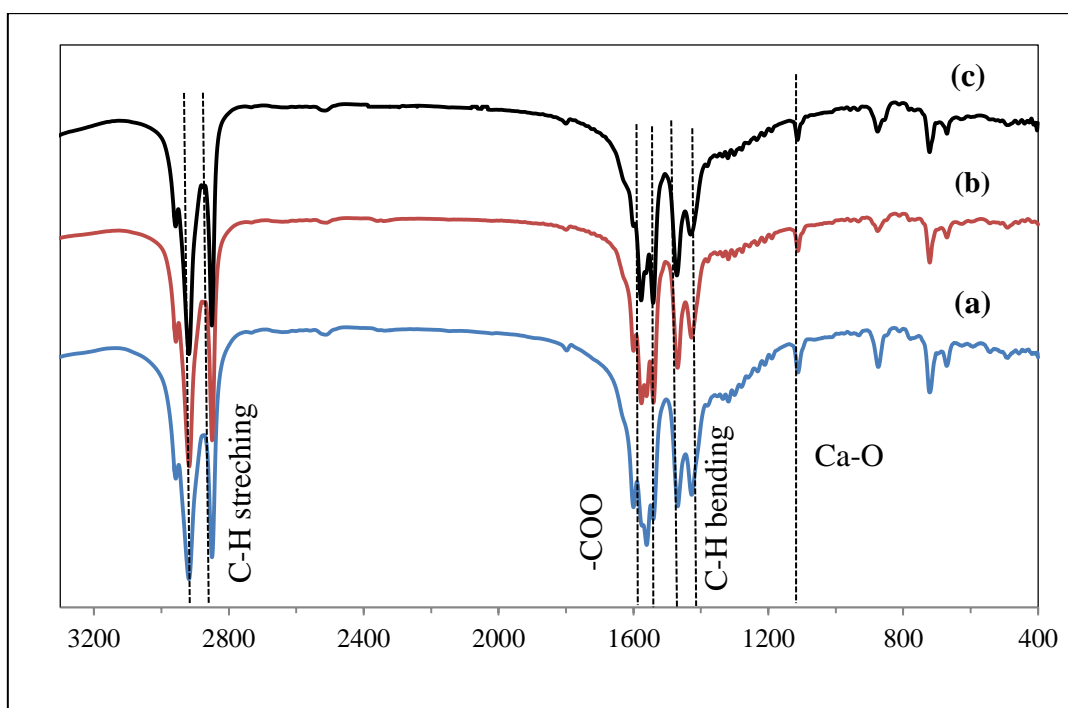
Figure 4.9 FTIR of the precipitated CaCO$_3$ at different incubation temperature a.) 30 ℃, b.) 60 ℃ and c.) 90 ℃

The surface hydrophobicity of precipitated $CaCO_3$ at incubation temperature of 60 and 90 ºC ware characterized by contact angle measurement. The contact angle was used to measure the extent of hydrophobic character of precipitated $CaCO_3$ surfaces. Precipitated $CaCO_3$ particles prepared from 2 mM of initial $Ca(OH)_2$ concentration with carbonation temperature of 30 ºC after drying at 110 ºC for 24 h are shown in Figure 4.10a and 4.10b, respectively. The contact angle of precipitated $CaCO_3$ at incubation temperature of 60 and 90 ºC are 153±1 and 152±3 degree, respectively, indicating super hydrophobic character. Although the SEM images (Figure 4.7) showed that the increasing of incubating temperature, particles size are almost the same as 300±41 nm to 380±80 and 400±96 nm. The property of precipitated $CaCO_3$ particles was still super hydrophobic property. The contact angle of precipitated $CaCO_3$ particles are almost the same, it probably the minor influence of incubation temperature so the particles shape and size were quite changed.
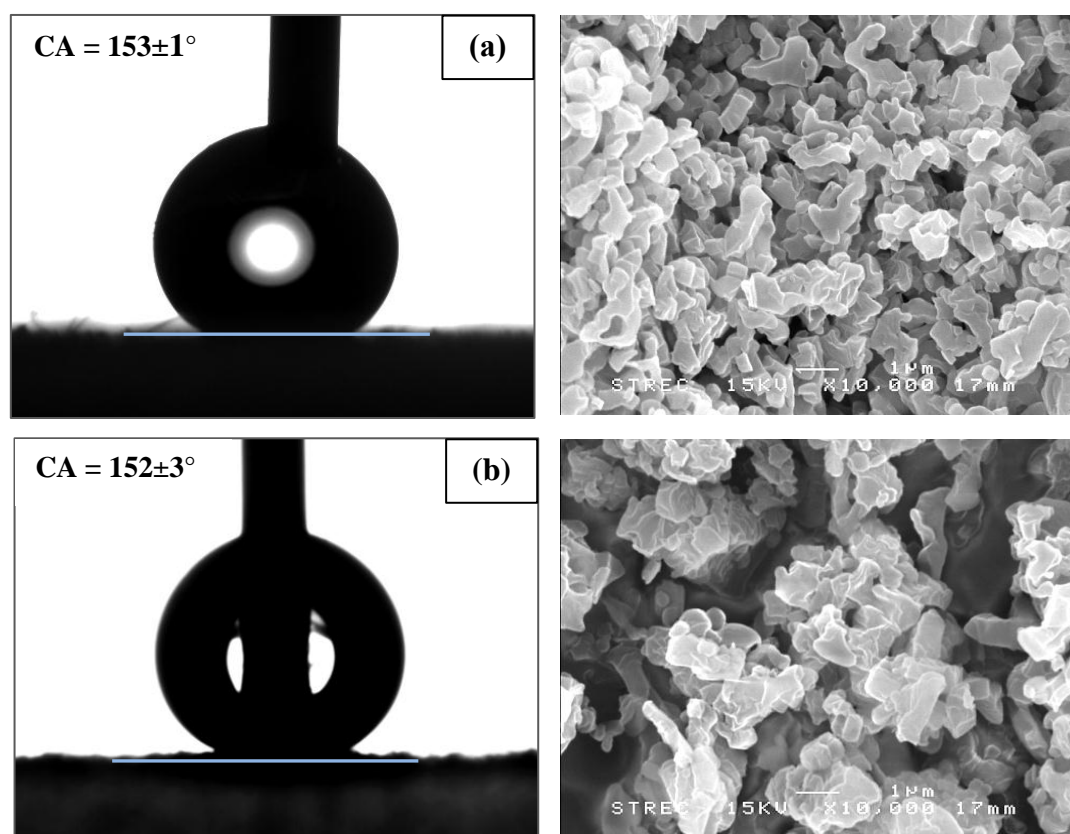
Figure 4.10 Contact angle on calcium carbonate products prepared at different incubation temperature a.) 30 ºC, b.) 60 ºC and c.) 90 ºC

4.3 Effect of carbonation temperature

Figure 4.11 shows the morphology of the precipitated $CaCO_3$ particles prepared at the carbonation temperature of 30, 60 and 90 ºC where the initial $Ca(OH)_2$ concentration ,incubation temperature and total CO_2/N_2 flow rate (1:1, v/v) were kept constant at 2 mM, 30 ºC and 0.2 L/min, respectively. The morphology of precipitated $CaCO_3$ obviously changed from the small particles to needle-like particles with increasing the carbonation temperature. The uniform small particles were formed at 30 ºC whereas the both of needle-like particles and the small particles were formed at 60 ºC and 90 ºC. The length and the diameter of the needle-like particles were increased when the carbonation temperature increased from 60 ºC to 90 ºC. It could be also seen that increase in carbonation temperature favored agglomeration of the small calcite particles which agree well with other researches on the influence of carbonation temperature [38]. They were found the tendency of agglomeration which was accelerated with increase in temperature resulting into a layered structure at 230 °C. The sizes of precipitated $CaCO_3$ particles were analyzed from image processing program. The uniform small particles, which were 300 nm, were obtained from carbonation temperature of 30 ºC (Figure 4.11a). With further increase in carbonation temperature to 60 ºC (Figure 4.11b.) and 90 ºC (Figure 4.11c), the mean diameter of needle-like particles were significantly increase from 220 nm and 900 nm which were mixed with small particles.

The increase in the particle size with temperature increase can also be explained by the competition existing between the nucleation and crystalline growth phases occurring in the $CaCO_3$ crystallization process which is dependent on the temperature changes. Indeed, at low temperatures, the nucleation rate is stronger than that of crystalline growth and the generated particles are of small size. On the other hand, when the temperature increases, the crystalline growth dominates thus leading to the production of particles of larger size. These results agree with those of Vucak et al [39] who studied the precipitation of calcium carbonate and concluded that the temperature increase during the $CaCO_3$ crystallization process led to particles of large size formed by sintering of nuclei obtained during the nucleation phase and also their growth. These results are nevertheless in disagreement with those of Yu et al [40]

who explained that at high temperature, the solubility of calcite is increased, resulting in CaCO$_3$ particles of reduced size.

The increase particles of larger size were also agree-well with Romuald [36]. They can observe that two polymorphic CaCO$_3$ species were produced, calcite and aragonite. However, the occurrence of the aragonite is not observed up to 80 ℃ where its size does not change significantly when the temperature increases to 100℃. They seem that aragonite is less sensitive to small temperature change such as ΔT of 20 ℃. Wider temperature variation could lead to significant changes in the aragonite particle size.

It is known that the solubility of calcite increases when the temperature is augmented. The particle regions with high surface energy such as the crystallite tops and edges dissolve readily in order to minimize the surface energy which results in a drastic morphology changes. These results are in agreement with those of Yu et al [40] who carried out the synthesis of the calcium carbonate particles by precipitation in aqueous phase while varying the temperature of reaction medium.

The relation between carbonation temperature and particles size could explain from the solution below:

$$B^0 = k(T)\, \omega^l \, M^j \, s^i$$

where B^0 =   surface reaction (integration) rate

   k   =   rate constant (function of temperature)

   ω =   a measure of mechanical

   M   =   the suspension density

   s   =   the degree of supersaturation

The surface reaction rate is increase by temperature level, at higher temperatures its rate would increase more, relative to the diffusion rate, resulting in a large particles size [48].
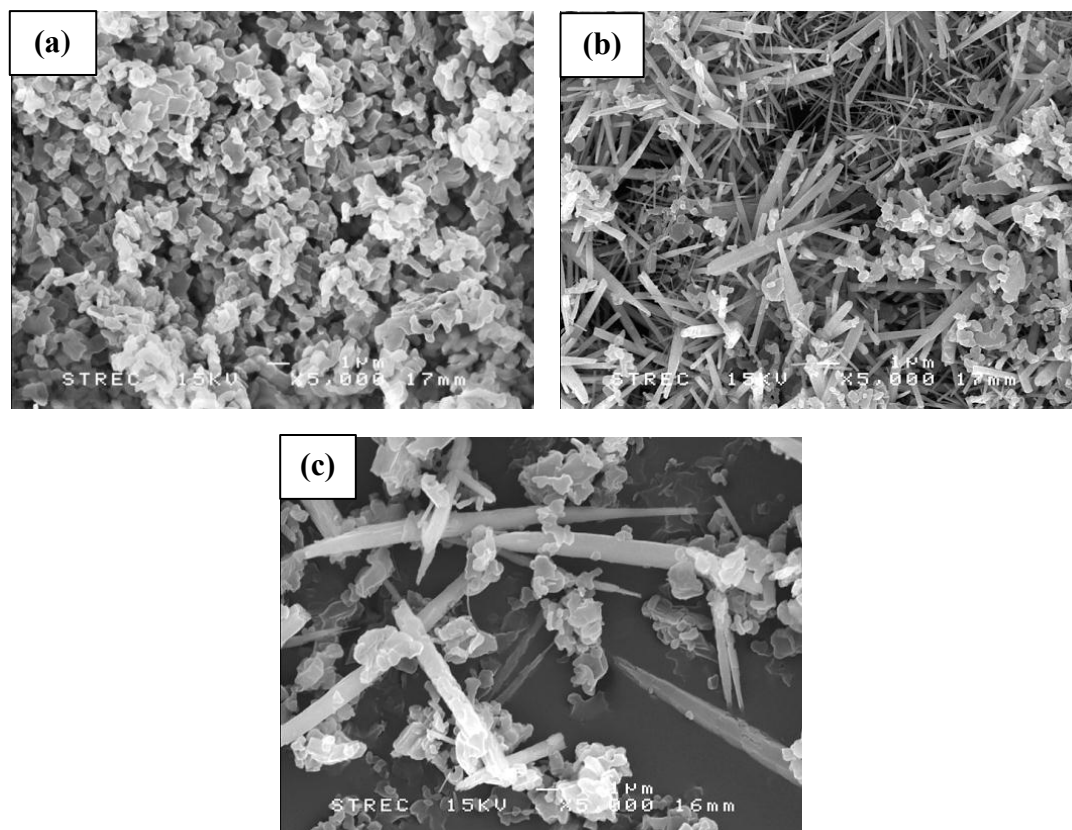
Figure 4.11 Typical SEM images of precipitated $CaCO_3$ particles prepared at different carbonation temperature (a) 30 ºC, (b) 60 ºC and (c) 90 ºC

In order to confirm the crystal structure of precipitated $CaCO_3$ from different carbonation temperature, X-ray diffraction was performed. Figure 4.12 illustrates X-ray diffreaction patterns of precipitated $CaCO_3$ from constant initial $Ca(OH)_2$ concentration of 2 mM and constant incubation temperature of 30 ºC at different carbonation temperature. It can be seen that the morphology of $CaCO_3$ changed with increase in carbonation temperature from 30, 60 and 90 ºC. Typical XRD patterns of calcium stearate were detected at 2θ values of 20.3, 21.7, 23.1 and 26.3 deg. Similar XRD pattern revealing the existence of calcium stearate was also reported by Mehmet et al [30].The patterns indicated the calcium stearate which was the bonding at $CaCO_3$ surface.

The peaks at 2θ values of 29.5, 35.9, 39.5 and 43.2 deg. are the pattern of calcite morphology [29] which are ascribed to [104], [110] and [113]. The peaks are at 2θ value of 26.2, 27.2, 33.1, 36.2, 37.2, 37.8, and 38.4 deg. are the pattern of

aragonite morphology which are ascribed to [111], [021], [012], [200], [031], [112] and [130], respectively [29]. It could be explained that XRD pattern of precipitated $CaCO_3$ particles at carbonation temperature of 30 ºC was the pattern of only calcite morphology whereas the carbonation temperature increase to 60 and 90 ºC some of calcite $CaCO_3$ particles changed to form the aragonite particles, resulting in XRD patterns of precipitated $CaCO_3$ at carbonation temperature of 60 and 90 ºC showed both of calcite and aragonite pattern.

The results in combination of XRD analysis reveal that the precipitated $CaCO_3$ prepared at 60 and 90 ºC composed of calcite and aragonite while only calcite was observed in the precipitated $CaCO_3$ prepared at 30 °C, which agree well with other researches on the influence of carbonation temperature [41].
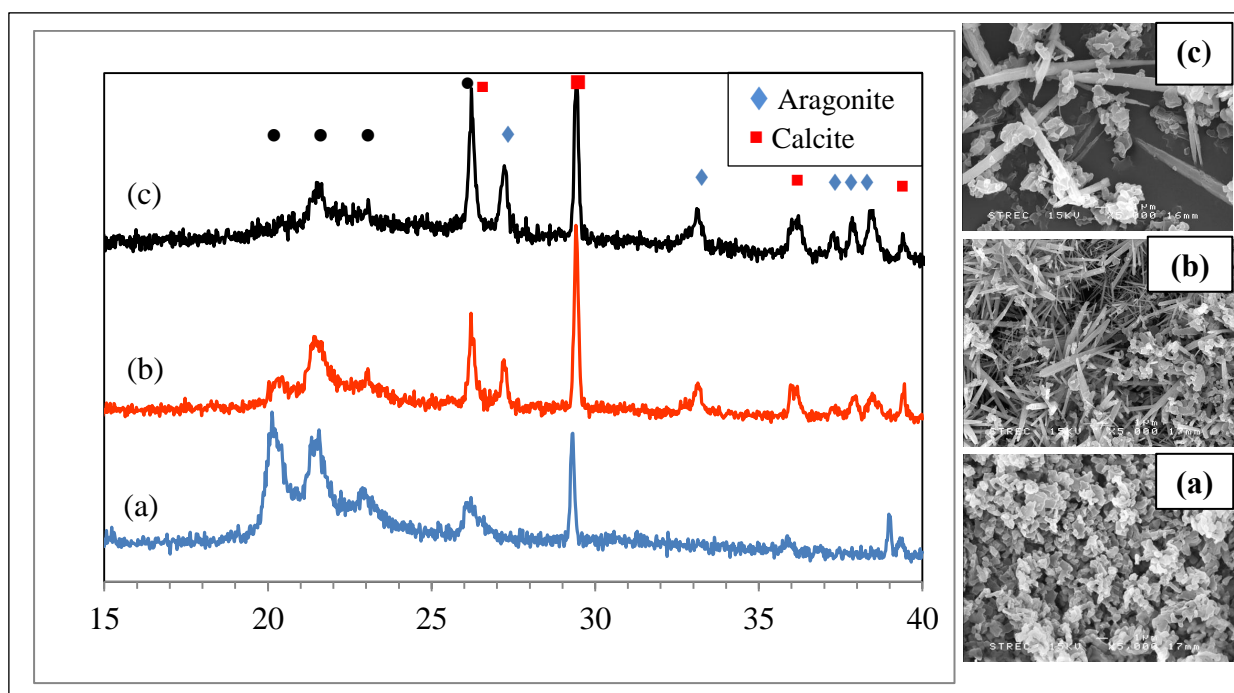
Figure 4.12 X-ray diffraction diagrams of products prepared at carbonation temperature (a) 30 ºC, (b) 60 ºC and (c) 90 ºC

The thermal vibrations can be explained the change of polymorphs and crystal structure with temperature. Aragonite's crystal lattice (Figure 4.13a) differs from that of calcite (Figure 4.13b) it causes different crystal shapes. Aragonite was coordinated to the nine oxygen atoms to the calcium atoms which is result that an increase in effective radii of the calcium atoms at high temperature [2].

Gabrielli has investigated the growth of aragonite and two growth models have been proposed [42]. In the first case, primary aragonite appeared as isolate thin needles with their growth along their c-axis. In the second case, aragonite crystals presented the aspect of irregular spindle subdivided in small cubic blocks. Our results on the growth of aragonite come along as first model. The aragonite grows via an oriented attachment of small aragonite particles [43] as shown in Figure 4.13b.
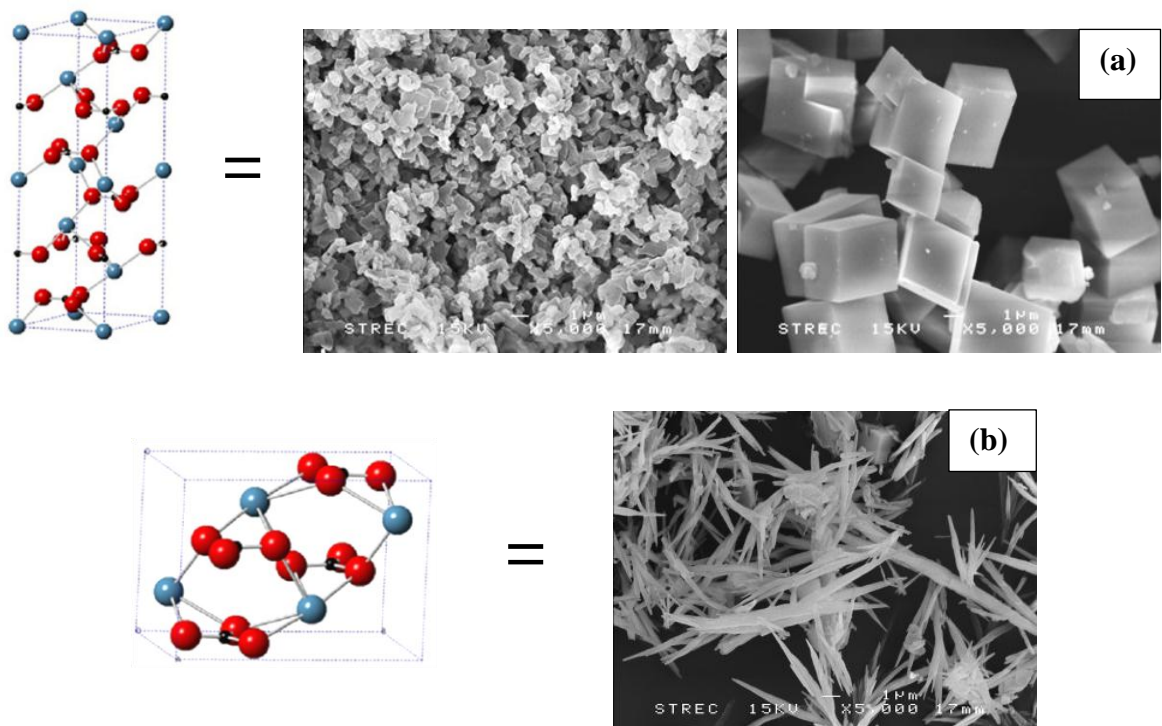
Figure 4.13 showed crystal lattice and morphology of a.) calcite b.) aragonite

Identification to the precipitates is further demonstrated by FTIR spectra as shown in Figure 4.14. The band at 713 cm^{-1} is the characteristic vibration band of calcite and aragonite while for aragonite, another typical absorption band assigned to the in plane bending vibration locates at 673 cm^{-1}. The vibration bands at 853 and 873 cm^{-1} can be attributed to the symmetric carbonate out-of-plane bending vibration of aragonite and calcite, respectively. The symmetric carbonate stretching vibration of aragonite at 1487 cm^{-1} can be observed from the FTIR spectra (b and c). The vibrational bands corresponding to calcite and aragonite are all found in the spectra of precipitated $CaCO_3$ at 60 ℃ and 90 ℃ while the vibration bands of calcite is found in the spectra of precipitated $CaCO_3$ at 30 ℃. The spectra reveal that the temperature increase to 60 and 90 ℃ signally causes the reinforcement of the band at 673 and 1487 cm^{-1} corresponding to aragonite. These results are in good agreement with those obtained by SEM images (Figure 4.11) and XRD pattern (4.12). Additionally, all of these spectra show the band centered at 1111 cm^{-1} is assigned to the O–Ca band of $(C_{17}H_{35}COO)_2Ca$. The characteristic bands of stearate group at 1541 and 1561 cm^{-1} can be assigned to the symmetric and asymmetric stretching vibration [32]. The peaks at 1427 and 1468 cm^{-1} are the peak of bending from long chain hydrocarbon. The strong peaks occurred around 2800 - 3000 cm^{-1} are characteristic of C-H symmetric and asymmetric stretching vibrations, which is the long chain of hydrocarbon from stearate, respectively. The results indicate that the organic additive was bound onto the surface of precipitated $CaCO_3$ [33],[34],[35],[36].

Figure 4.14 FTIR of the precipitated $CaCO_3$ at different carbonation temperature a.) 30 ºC, b.) 60 ºC and c.) 90 ºC

Figure 4.15 Contact angle on calcium carbonate products precipitated at the carbonation temperature of (a) 60 ºC and (b) 90 ºC
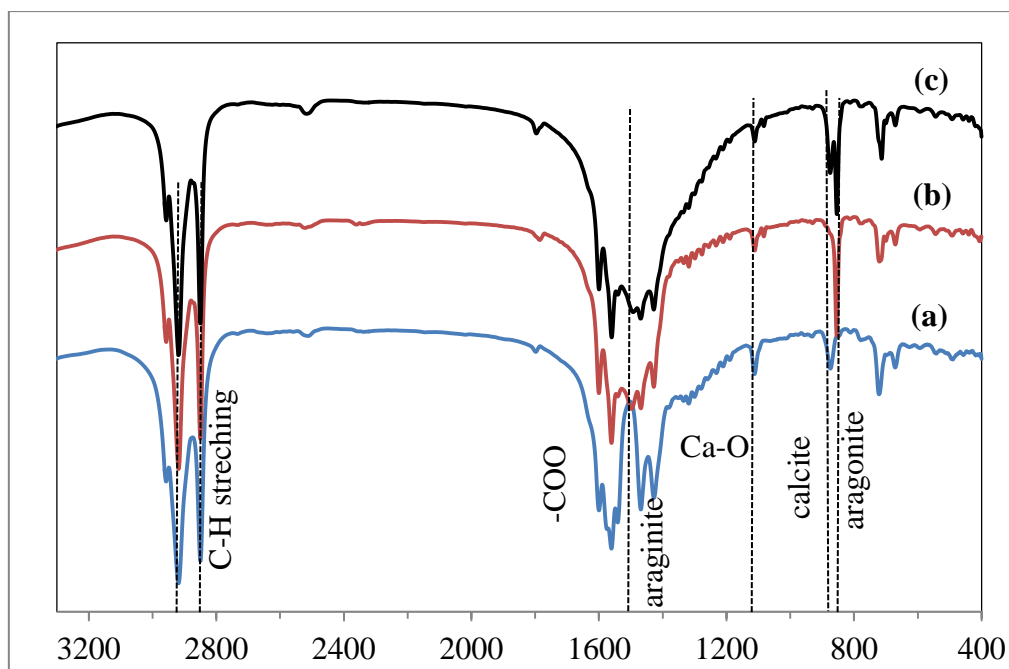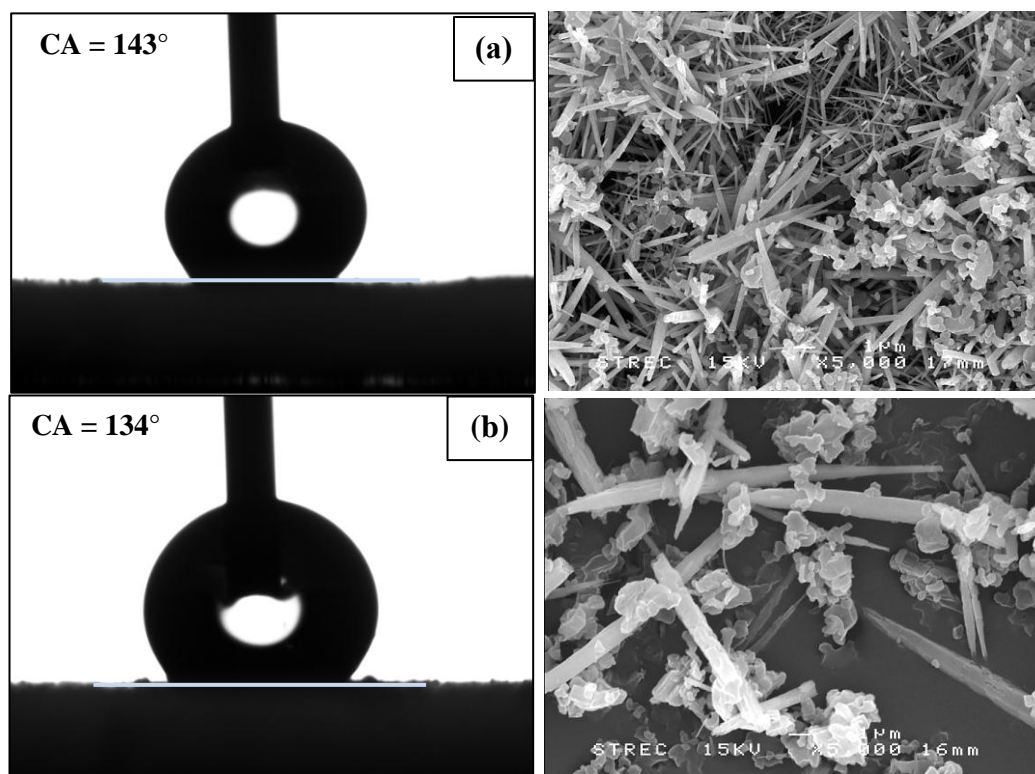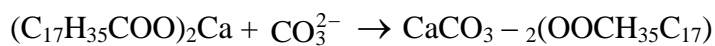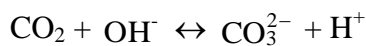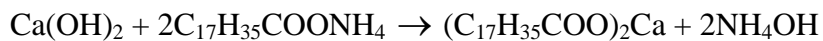
The surface hydrophobicity of precipitated $CaCO_3$ at carbonation temperature of 60 and 90 ºC ware characterized by contact angle measurement. The contact angle was used to measure the extent of hydrophobic character of precipitated $CaCO_3$ surfaces. Precipitated $CaCO_3$ particles prepared from 2 mM of initial $Ca(OH)_2$ concentration with carbonation temperature of 60 and 90 ºC after drying at 110 ºC for 24 h are shown in Figure 4.15a and 4.15b, respectively. The contact angle of precipitated $CaCO_3$ at the carbonation temperature of 60 and 90 ºC are 143±2 and 134±2 degree, respectively, indicating good hydrophobic character. Although the XRD analysis (Figure 4.12) showed the change of the morphology from rhombohedral calcite to orthorhombic aragonite, the property of precipitated $CaCO_3$ particles was still strong hydrophobic property. The contact angle values increase with decrease in carbonation temperature, it probably the size of precipitated $CaCO_3$ was increased. The contact value depend on the type of surface roughness, small particle size is related to high surface area which tends to be high roughness. The results are agree-well with Wenzel [44]. Wenzel has presented a theory for the effect of surface roughness on contact angles which has been widely accepted. He points out that within a given geometrical area a roughened surface will contain more actual surface area than will a smooth surface. It should be note that another one cause of decrease in contact angle values is the surface coverage. Crawford [48] indicated that the contact angle decrease with decrease in surface coverage. The carbonation temperature increase from 30 to 60 and 90 °C, it probably surface modifier activity decrease tends to decrease in surface coverage which cause the decrease of contact angle and hydrophobic property.

Precipitated $CaCO_3$ particles were synthesized and modified by carbonation process with an objective to manipulate hydrophobicity of $CaCO_3$ particles. The hydrophobic surface property of $CaCO_3$ particles could be manipulated by ammonium stearate ($C_{17}H_{35}COONH_4$) solution which was added into $Ca(OH)_2$ solution before carbonation process. 1 mM of stearic acid ($C_{17}H_{35}COOH$) was added into 200 ml hot de-ionized water to form suspension. Then, NH_4OH was introduced into suspension for help the stearic acid dissolved. This suspension was vigorously stirred for several minutes to obtain a saponification solution for using as organic substrate. The

different concentration of $Ca(OH)_2$ (1, 2, 3 and 4 mM) was added into the substrate. The mixture was incubated in order that Ca^{2+} can associate with the organic substrate to form chemical bond by interface recognition of molecules. The solution which is subject to bubbling of CO_2 gas mixture. CO_2 and N_2 were prepared with a designated volume ratio of 1:1 before introducing into the slurry with constant of total flow rate. CO_2 gas was disolved in to the high pH solution to form CO_3^{2-}. The reaction was undergone at different constant carbonation temperature (30, 60 and 90 ºC). The hydrophobic $CaCO_3$ crystals were formed and growth while pH value of slurry was decreased. The reaction was stopped when the final pH value of suspension was 7. The crystalline $CaCO_3$ particles was rinsed off for remove contaminating of organic substrates and then dried at 110 ºC in an oven to obtain the hydrophobic $CaCO_3$ product before characterization of the obtained solid sample.

$$C_{17}H_{35}COOH + NH_4OH \leftrightarrow C_{17}H_{35}COONH_4 + H_2O$$

$$Ca(OH)_2 + 2C_{17}H_{35}COONH_4 \rightarrow (C_{17}H_{35}COO)_2Ca + 2NH_4OH$$

$$CO_2 + OH^- \leftrightarrow CO_3^{2-} + H^+$$

$$(C_{17}H_{35}COO)_2Ca + CO_3^{2-} \rightarrow CaCO_3 - {}_2(OOCH_{35}C_{17})$$

$$Ca(OH)_2 + 2C_{17}H_{35}COOH + CO_2 \rightarrow CaCO_3 - {}_2(OOCH_{35}C_{17}) + H_2O \qquad (4.1)$$
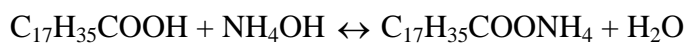
Theoretical yield of precipitated $CaCO_3$ at different carbonation temperature (30, 60 and 90 ºC) was defined based on the precipitation equation as shown in equation (4.1). To obtain 1 mole of precipitated $CaCO_3$, one mole of $Ca(OH)_2$ would completely react with 2 moles of stearic acid ($C_{17}H_{35}COOH$) . Therefore theoretical yield is defined as shown in equation (4.2). Meanwhile actual yield of preciptaed $CaCO_3$ products is defined in equation (4.3). It is an actual mass of precipiteated $CaCO_3$ after drying process. Therefore percent yield of precipitaed $CaCO_3$ is defined as a ratio of actual yield to theoretical yield as shown in equation (4.4).

Theoretical yield [g] = 1 × mol Ca(OH)$_2$ × MW.coated CaCO$_3$ $\qquad$ (4.2)

Actual yield [g] = Mass of precipitaed CaCO$_3$ $\qquad$ (4.3)

Percent yield [%] = (Actual yield/Theoretical yield) × 100% $\qquad$ (4.4)

Percent yields of precipitated CaCO$_3$ products were systematically investigated by varying the carbonation temperature. The percent yields of precipitated CaCO$_3$ products calculated by equation (4.4) were shown in Figure 4.16. With constant initial Ca(OH)$_2$ concentration of 2 mM, it was found that percent yield is dramatically increased from 49 % to 59 % with carbonation temperature. The results can suggested that due to high reaction temperature, the Brownian motion of ion (Ca^{2+}, CO_3^{2-}) and particle mobility are high enough to enhance the probability of ion collision and then of precipitation increase. [45]
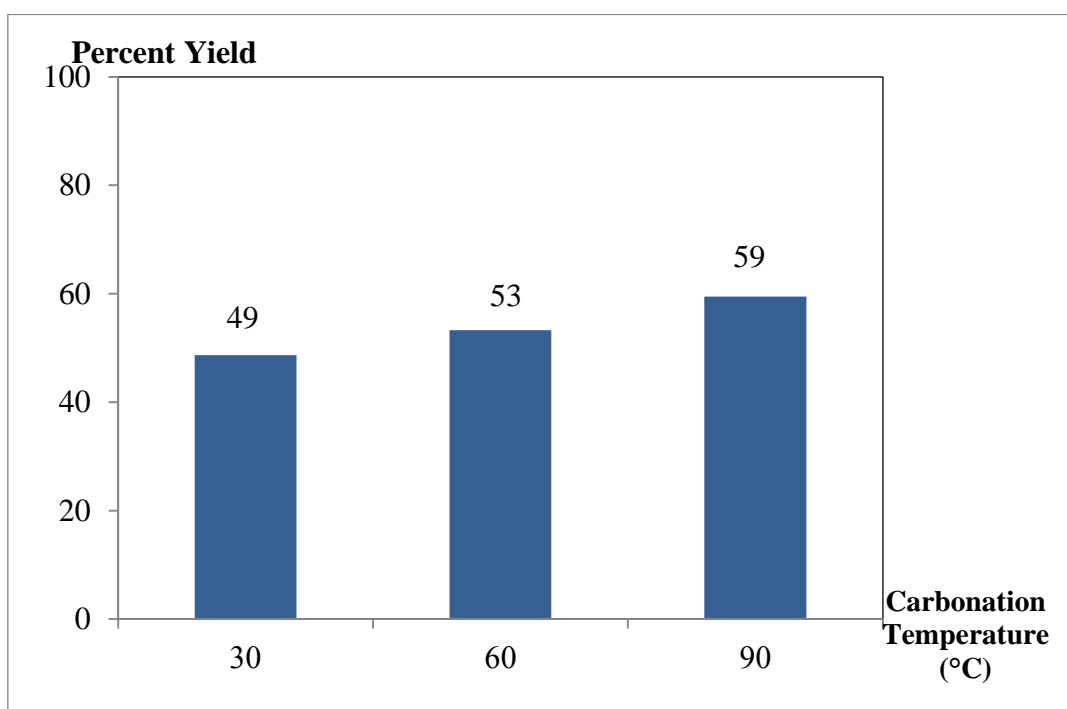
Figure 4.16 Change of synthesizing yield of precipitated CaCO$_3$ particles synthesized at different carbonation temperature

4.4 Effect of total CO_2/N_2 flow rate

The morphology of precipitated $CaCO_3$ particles prepared at different total CO_2/N_2 flow rate is shown in Figure 4.17, where the initial $Ca(OH)_2$ concentration, incubation temperature, carbonation temperature and stirring rate were kept constant at 4 mM, 30 ºC, 30 ºC, 400 rpm, respectively. It can be seen from Figure 4.17a that the large rhombohedral calcite particles significantly decreased with increase in total CO_2/N_2 flow rate from 0.1 to 0.2 L/min. The particle size analysis based on image processing program ,the small particle size decrease from 460 nm to 280 nm and also the large rhombohedral calcite decrease from 3.7 μm to 3.1 μm when the total CO_2/N_2 flow rate increase. The change of precipitated size with flow rate may be attributed to the dissolution rate of CO_2 at different conditions. The increase of flow rate would enhance the gas–liquid mass transfer and dissolving of CO_2 as resulting in the accumulation of H^+, HCO_3^-, CO_3^{2-} ions, thus increasing the supersaturation of solution. The high supersaturation leads to the quick nucleation and precipitation, which limits the growth. So the small particles were obtained and became the major size at the high flow rate which agree well with other researches on the influence of gas flow rate on the carbonation of $CaCO_3$ [46],[47].
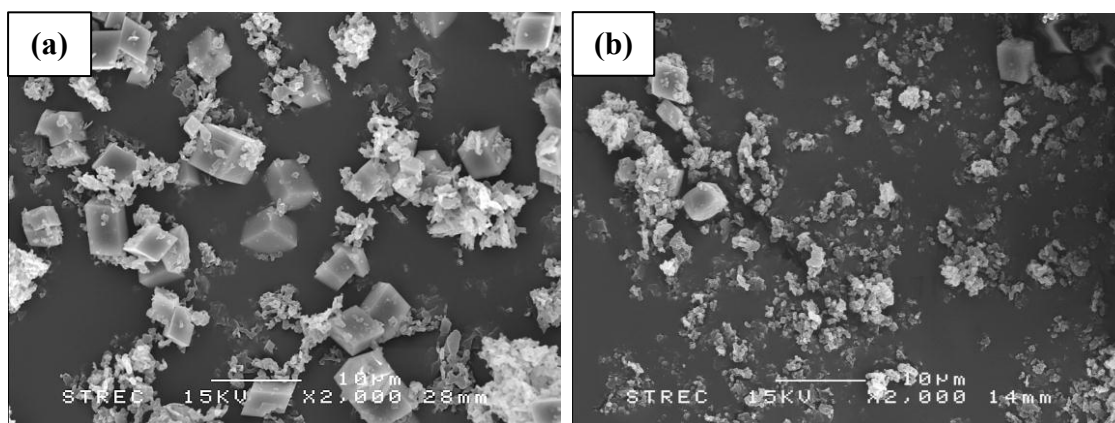
Figure 4.17 SEM images of $CaCO_3$ particles prepared at different total CO_2/N_2 flow rate (a) 0.1 L/min and (b) 0.2 L/min
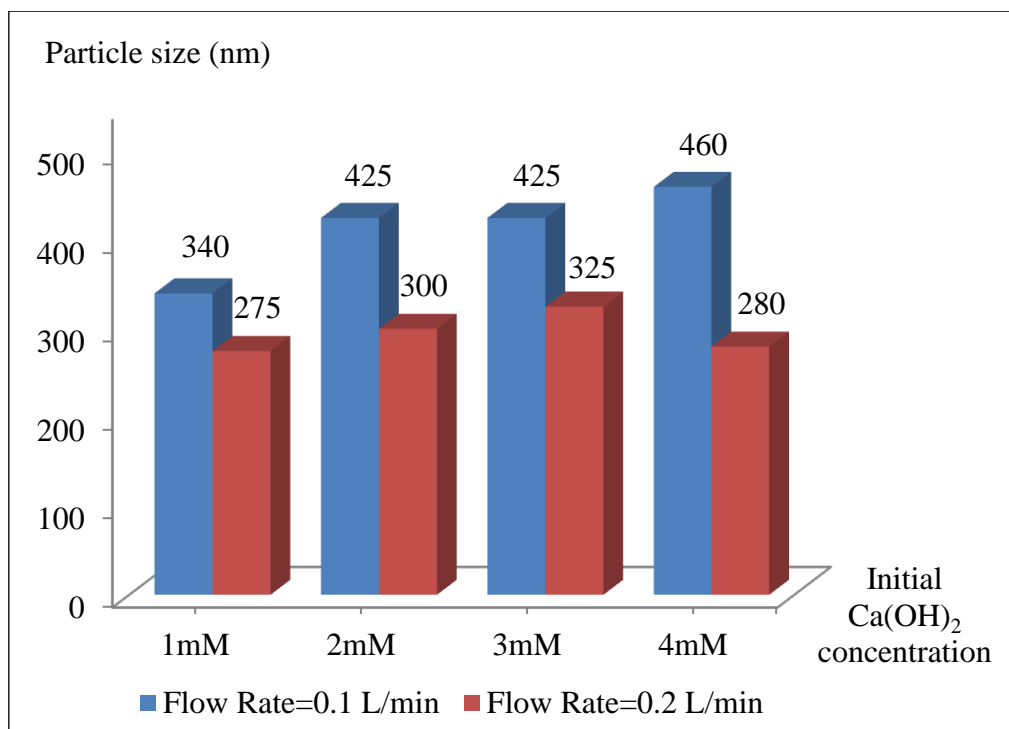
Figure 4.18 Change of particle size of precipitated $CaCO_3$ particles synthesized at different total CO_2/N_2 flow rate

Meanwhile, the precipitation of $CaCO_3$ at different total CO_2/N_2 flow rate and different initial $Ca(OH)_2$ concentration was also analyzed and reported as Figure 4.17. It was found that the total CO_2/N_2 flow rate at all initial $Ca(OH)_2$ concentration (1, 2, 3 and 4 mM) increased, the small particle size of precipitated $CaCO_3$ all decreased which were shown in Figure 4.18. The results could be confirmed the influence of total CO_2/N_2 flow rate on the particle size of precipitated $CaCO_3$. The precipitation from initial $Ca(OH)_2$ concentration of 4 mM at total gas flow rate of 0.2 L/min. show the smaller particle size than the precipitation from initial $Ca(OH)_2$ concentration of 2 mM and 3 mM at the same gas flow rate because there are small particle with 280 nm and the large rhombohedral calcite particle with 3.1 μm.

Figure 4.19 show the XRD patterns of the precipitated products which was synthesized at different total CO_2/N_2 flow rate (1:1, v/v) whereas initial $Ca(OH)_2$ concentration, incubation temperature and carbonation temperature were kept constant at 4 mM, 30 ºC and 30 ºC ,respectively. It should be noted that the same XRD patterns at 2θ values of 29.5, 35.9, 39.5, 43.2, 47.2, 47.6, 48.5, 56.6 and 57.4

deg. were calcite structure of $CaCO_3$ which are ascribed to [104], [110], [113], [202], [024], [018], [116], [121] and [122], respectively [29],. The calcite patterns appear on both products with the short XRD patterns of calcium stearate were also detected at 2θ values of 20.3, 21.7, 23.1 and 26.3 deg. which are shown at all products.
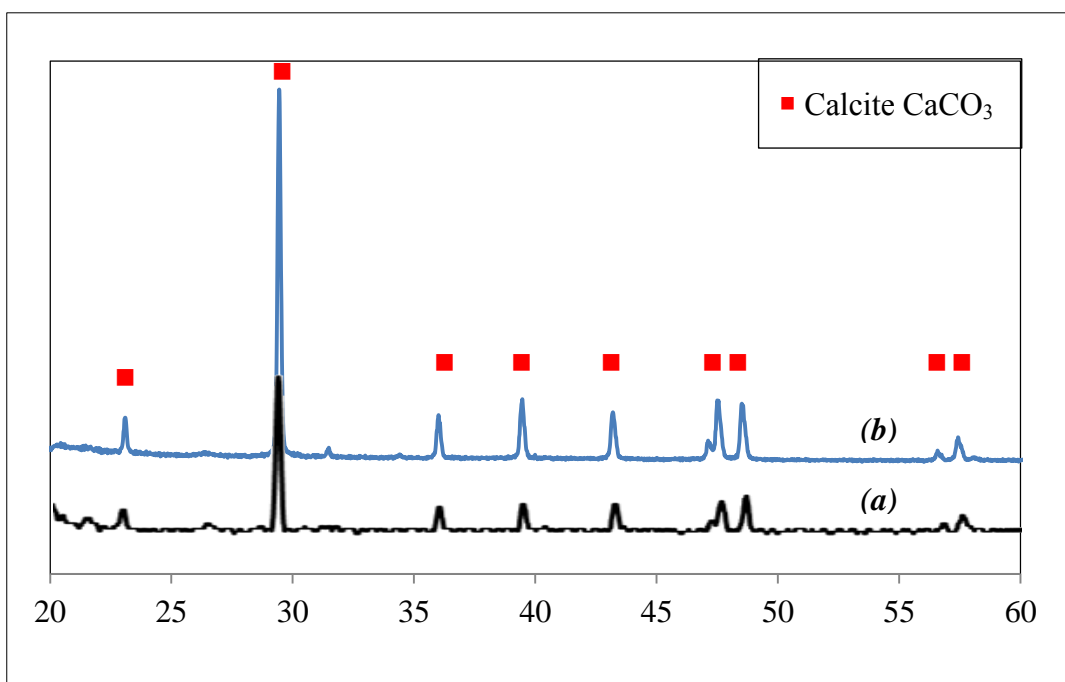
Figure 4.19 X-ray diffraction diagrams of products prepared at total CO_2/N_2 flow rate of (a) 0.1 L/min and (b) 0.2 L/min

Figure 4.20 shows FTIR spectra of precipitated $CaCO_3$ at initial $Ca(OH)_2$ concentrations of 2 mM at constant carbonation temperature of 30 ºC with different CO_2/N_2 flow rate (0.1 L/min, 0.2 L/min) prepared by KBr in comparison with pure $CaCO_3$ particles. There are three fundamental IR active bands of $CaCO_3$ in the spectra [30]. The fundamental bands at 712, 874 and 1420 cm^{-1} are in-plane-bending, out-of-plane bending, and the asymmetric stretching, respectively. The combination bands are also observed at 1797, 2512, and 2917 cm^{-1} [31]. The large vibrational band from 1250 – 1600 cm^{-1} contains the fundamental degenerate stretching frequency of carbonate at 1420 cm^{-1}. For the precipitated $CaCO_3$, the absence of a strong peak at 1703 cm^{-1} and broad peak around 2800 – 3200 cm^{-1} of pure stearic acid which corresponds to -C=O stretching and O-H stretching of carboxylic acid group. This

peak not appears at the precipitated $CaCO_3$ because carboxylic acid group was changed to carboxylate group. The characteristic bands at 1541 and 1561 cm^{-1} can be assigned to the symmetric and asymmetric stretching vibration of carbonate group [32]. The peaks at 1427 and 1468 cm^{-1} are the peak of bending from long chain hydrocarbon. The strong peaks occurred around 2800 - 3000 cm^{-1} are characteristic of C-H symmetric and asymmetric stretching vibrations, which is the long chain of hydrocarbon from stearic acid, respectively.

It also showed the band centered at 1111 cm^{-1} which is assigned to the O–Ca band of $(C_{17}H_{35}COO)_2Ca$. This band indicates that the organic additive was bound onto the surface of precipitated $CaCO_3$ [33],[34],[35],[36]. Moreover, The peaks of precipitated $CaCO_3$ from 0.2 L/min flow rate has more effect of stearate than the 0.1 L/min because the sharp peaks at 1554 and 1563 cm^{-1} exhibited higher. These results are agree-well with the results from SEM images. The SEM image of precipitated $CaCO_3$ from 0.2 L/min. showed more small particles than the SEM image from flow rate of 0.1 L/min. The absence of large rhombohedral calcite indicated the interaction of stearate on the $CaCO_3$ surface resulting in the size controlling.
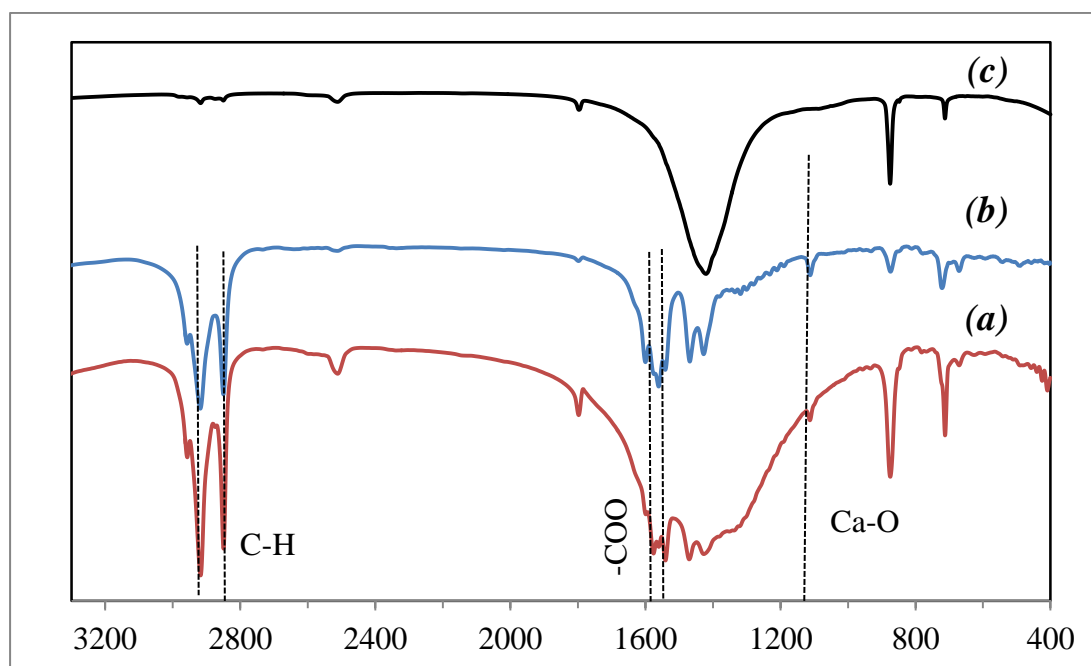
Figure 4.20 FTIR of the precipitated $CaCO_3$ at total CO_2 /N_2 flow rate of a.) 0.1 L/min, b.) 0.2 L/min and c.) pure $CaCO_3$

The surface hydrophobicity of precipitated $CaCO_3$ at total CO_2/N_2 flow rate (1:1, v/v) of 0.1 and 0.2 L/min ware characterized by contact angle measurement. The contact angle was used to measure the extent of hydrophobic character of precipitated $CaCO_3$ surfaces. Precipitated $CaCO_3$ particles prepared from 4 mM of initial $Ca(OH)_2$ concentration with constant incubation and carbonation temperature of 30 ºC after drying at 110 ºC for 24 h are shown in Figure 4.21a and 4.21b, respectively. The contact angle of precipitated $CaCO_3$ at flow rate of 0.1 and 0.2 L/min are 154±2 and 153±2 degree, respectively, indicating super hydrophobic property. Although SEM analysis (Figure 4.17) showed that the large particles which are rhombohedral calcite significantly decreased with increase in total CO_2/N_2 flow rate, the property of precipitated $CaCO_3$ particles was still super hydrophobic property. The contact angle values are similar, it probably the amount of stearic acid which was used as surface modifier cover $CaCO_3$ surface with the same quantity.
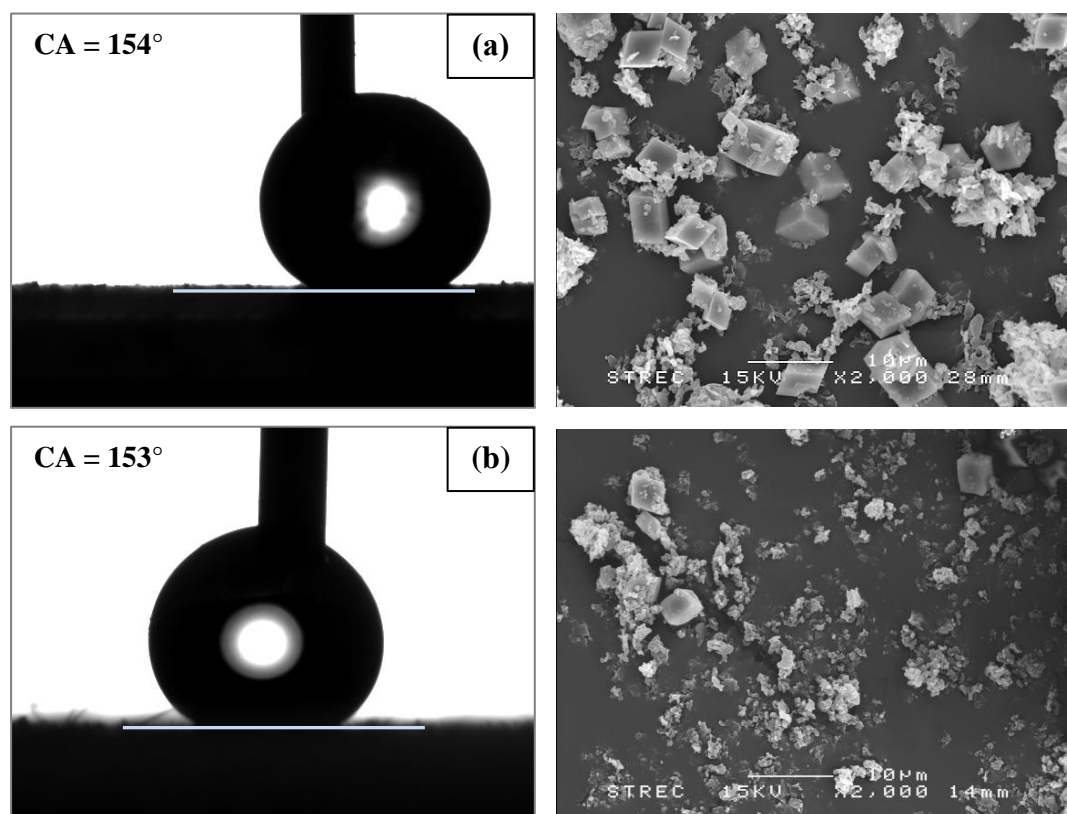
Figure 4.21 Contact angle on calcium carbonate products precipitated at the total CO_2/N_2 flow rate of (a) 0.1 and (b) 0.2 L/min

4.5 Kinetics modeling

In order to investigate the precipitated process of $CaCO_3$ using stearic acid as a surface modifier, the kinetics model is the pseudo first-order has been used to fit the experiment data.

Pseudo-first-order model

The pseudo-first-order reaction depends on the concentration of only one reactant. The other reactants in the rate equation are present in the great excess and the other one is used as additive in the reaction mixture that its effect is not seen which can be expressed following as (4.5):

$$\frac{dC}{dt} = -kt \tag{4.5}$$

The above equation (4.5) is integrated for the boundary condition at t = 0 to t = t and $C=C_0$ to C=0 it may be rearranged for straight-line data plots as shown in Eq. (4.6):

$$\ln C = \ln C_0 - kt$$

$$\ln \frac{C}{C_0} = -kt \tag{4.6}$$

where C_0 =   concentration of $Ca(OH)_2$ solution at the beginning of the carbonation reaction

   C   =   concentration of $Ca(OH)_2$ solution after the carbonation reaction at time (t)

   k   =   the rate constant of the pseudo-first-order carbonation reaction

   t   =   time (sec^{-1})

Table 4.2 Rate constant and R square value of pseudo-first-order model for carbonation reaction at different temperatures

T(°C)	Pseudo-First order model	
	k (sec-^{1})	R^2
30	0.0159	0.9636
60	0.0180	0.9958
90	0.0204	0.9903

The k values for carbonation reaction were determined from the plot of ln $\dfrac{C}{C_o}$

against t.

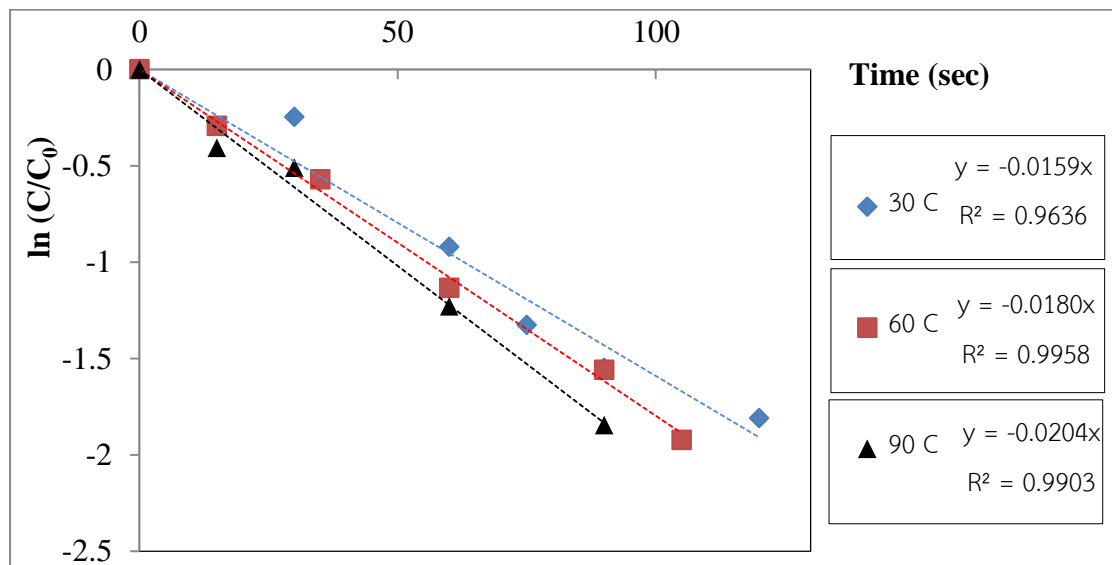**Figure 4.22** Pseudo-first-order plots for the carbonation reaction of Ca(OH)$_2$ to CaCO$_3$ at different temperature: (◆) 30 °C, (■) 60 °C and (▲) 90 °C

Furthermore, the activation energy (E_a) for carbonation reaction was possible calculated according to the Arrhenius equation based on the obtained k values in Table 4.2. Arrhenius equation is as follows:

$$k = Ae^{\left(\frac{-E_a}{RT}\right)}$$ (4.7)

where *A* is the frequency factor (min^{-1}), E_a is the activation energy (kJ /mol), *R* is the ideal gas constant (J/mol*K) and *T* is the absolute temperature (K).

Eq. (4.7) can be converted into Eq. (4.8) by taking logarithm:

$$\ln k = \ln A - \frac{E_a}{RT} \tag{4.8}$$

Thus, E_a could be determined from the slope of the line plotting ln k versus 1000/T as shown in Figure 4.23. From the results, the estimated E_a for the carbonation of $Ca(OH)_2$ to $CaCO_3$ was 3.79 kJ/mol.
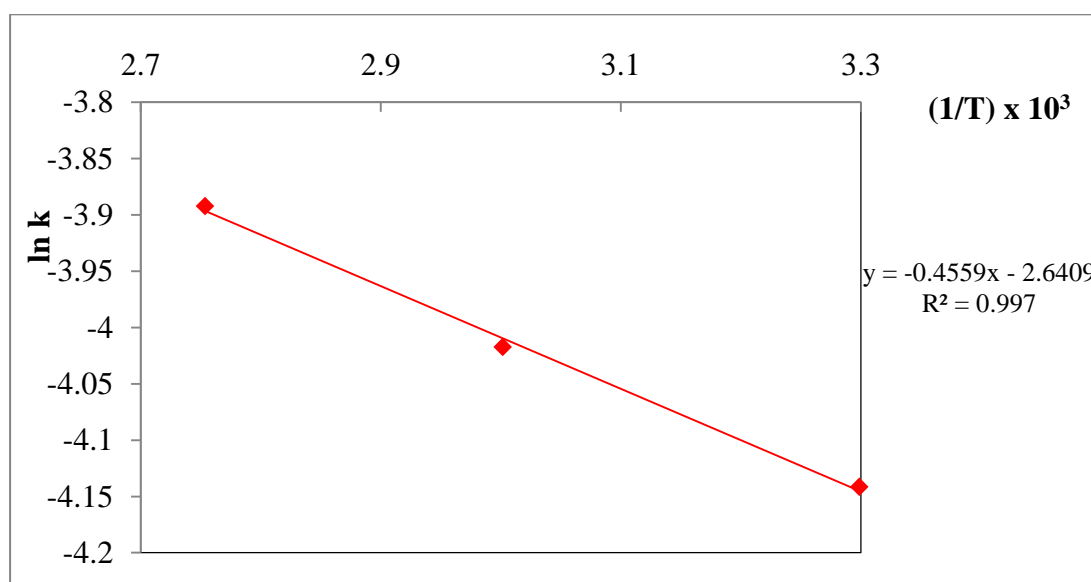
Figure 4.23 Correlation between ln k and 1000/T of precipitated $CaCO_3$ from carbonation reaction

4.6 Thermodynamic studies

Study of the temperature dependence of carbonation reaction provides valuable information regarding the energetic changes during carbonation reaction. The equilibrium carbonation coefficient (K_c) for the carbonation reaction was used for calculate the standard Gibbs free energy change (ΔG^0), standard enthalpy change (ΔH^0), and standard entropy change (ΔS^0) by the following equation:

$$\Delta G^0 = -RT \ln K_c \qquad (4.9)$$

$$\Delta G^0 = \Delta H^0 - T\Delta S^0 \qquad (4.10)$$

The combination of Eq. (4.9) and (4.10) yield:

$$\ln K_c = \frac{-\Delta G^0}{RT} = \frac{\Delta S^0}{R} - \frac{\Delta H^0}{RT} \ ; \qquad (4.11)$$

Where R is the universal gas constant (8.314 J/mol*K), T is the temperature (K) and K_c is the equilibrium carbonation coefficient. Gibbs free energy change of carbonation (ΔG^0) was defined using ln K_c values for different temperatures. According to Eq. (4.11), ΔH^0 and ΔS^0 parameters can be obtained from the slope and intercept of the liner plot of ln K_c against 1/T in Figure 4.23.

The thermodynamic parameters are listed in Table 4.3. The positive values of ΔH^0 and the negative values of ΔG^0 confirmed the endothermic and spontaneous nature of carbonation process.

Table 4.3 Thermodynamic parameters of carbonation reaction at different temperature

ΔG^0 (kj/mol)			ΔH^0	ΔS^0
30°C	**60°C**	**90°C**	**(kj/mol)**	**(KJ/mol-K)**
-10.438	-11.127	-11.752	+3.79	+0.022

CHAPTER VI

CONCLUSION AND RECOMMENDATIONS

5.1 Conclusion

In this thesis, synthesis of hydrophobic $CaCO_3$ nanoparticles using stearic acid as surface modifier was set as the main objective. Hydrophobic $CaCO_3$ particles could be prepared by bubbling CO_2/N_2 gas into precursor solution containing $Ca(OH)_2$, $C_{17}H_{35}COOH$ and NH_4OH. The experimental results showed that the initial $Ca(OH)_2$ concentration, carbonation temperature and total CO_2/N_2 flow rate would exert significant effect on characteristics of precipitated $CaCO_3$ particles.

Uniform-sized $CaCO_3$ particles with negligible impurity could be synthesized under a certain conditions of 2 mM of initial $Ca(OH)_2$ concentration. With this optimal concentration, introduction of surface modifier could control the size of the precipitated $CaCO_3$ particles. $CaCO_3$ with 300 nm mean diameter and 49 % synthesizing yield could repeatedly be synthesized. In addition, XRD analysis could confirm the presence of calcite polymorph. The surface modifier which was bound onto the surface of precipitated $CaCO_3$ would be attributed to hydrophobic property of particles. The contact angle was increased to 153±2 degree when compared with pure $CaCO_3$ which has 111±6 degree.

The carbonation temperature was another factor affecting the formation of calcite and aragonite. Needle-like aragonite with diameter of 220 and 900 nm were precipitated at 60 and 90 °C, respectively. The contact angle of precipitated $CaCO_3$ at the carbonation temperature of 60 and 90 ºC are 143±2 and 134±2 degree, respectively, indicating good hydrophobic property.

The large rhombohedral calcite particles significantly decreased with an increase in total flow rate of CO_2/N_2 which was varied in range of 0.1 to 0.2 L/min. XRD and FT-IR analyses also showed the increase of large particles with respect to a

decrease in total flow rate of CO_2/N_2. The contact angle values of 153-154 degree was however insignificantly affected.

The incubation temperature could exert a certain degree of influence on property of synthesized $CaCO_3$ particles. The mean diameter of $CaCO_3$ particles was increased from 275 nm to 380 nm and 400 nm with an increase in incubation temperature. The contact angles of precipitated $CaCO_3$ particles was insignificantly affected by the incubation temperature.

5.2 Recommendations

Facile synthesis of hydrophobic calcium carbonate ($CaCO_3$) had been conducted via aqueous reaction route incorporated with stearic acid. The smallest particles size of calcite and aragonite $CaCO_3$ are about 275 and 220 nm, respectively. We could conclude the interaction between $CaCO_3$ surface and the surface modifier which changed the surface property from hydrophilic to hydrophobic. The influence of initial $Ca(OH)_2$ concentration, incubation temperature, carbonation temperature and total CO_2/N_2 flow rate had already been examined.

The recommendations for future work are the application of precipitated $CaCO_3$ is utilization as filler incorporated in some composite materials such as paper, plastics, paint and rubber. Hydrophobic $CaCO_3$ particles with uniform size and high purity synthesized in this thesis. Mixed with polymer should be investigated. Scale up of this synthesizing process should also be examined.

REFERENCES

[1]   Wang, C., Sheng, Y., Zhao, X., Pan, Y., and Wang, Z., Synthesis of hydrophobic $CaCO_3$ nanoparticles. <u>Materials Letters</u> 60,6,(2006): 854-857.

[2]   Han, Y.S., Hadiko, G., Fuji, M., and Takahashi, M., Factors affecting the phase and morphology of $CaCO_3$ prepared by a bubbling method. <u>Journal of the European Ceramic Society</u> 26,4,(2006): 843-847.

[3]   Adams, H.R., Veterinary pharmacology and therapeutics. (Iowa State University Press, 2001.

[4]   Wang, C., Sheng, Y., Zhao, X., Zhao, J., Ma, X., and Wang, Z., A novel aqueous-phase route to synthesize hydrophobic $CaCO_3$ particles in situ. <u>Materials Science and Engineering</u>, 27,1,(2007): 42-45.

[5]   Chen, X., Zhu, Y., Guo, Y., Zhou, B., Zhao, X., Du, Y., Lei, H., Li, M., and Wang, Z., Carbonization synthesis of hydrophobic $CaCO_3$ at room temperature. <u>Colloids and Surfaces A</u> 353,2,(2010): 97-103.

[6]   Hafiz, W.M., and Harun, W., Effect of nano calcium carbonate on epoxy composite reinforced recycle rubber.

[7]   Structure Trigonal, C., and point Non-flammable, F., Alka-Seltzer Antacid.

[8]   Cao, G.F., and Yu, W.W., A Designing of the Manufacturing Facility for Disposing of Greenhouse Gases. <u>Advanced Materials Research</u> 503,(2012): 211-214.

[9]   Herbert A. Lieberman, Leon Lachman, Joseph B. Schwartz (1990). <u>Pharmaceutical Dosage Forms: Tablets.</u> New York: Dekker. p. 153. ISBN 0-8247-8044-2

[10]   Porter, S.M., Seawater chemistry and early carbonate biomineralization. <u>Science</u> 316,5829,(2007): 1302-1302.

[11] Runnegar, B., Shell microstructures of Cambrian molluscs replicated by phosphate. Alcheringa 9,4,(1985): 245-257.

[12] Geyssant, J., The limestones-development and classification: Calcium Carbonate. Springer (2001):15-30.

[13] Emken, E., Metabolism of dietary stearic acid relative to other fatty acids in human subjects. The American journal of clinical nutrition 60,6, (1994): 1023S-1028S.

[14] Roberts, J.D., and Caserio, M.C., Basic principles of organic chemistry. : WA Benjamin, Inc., 1977.

[15] Snyder, C.H., Extraordinary Chemistry of Ordinary Things. : John Wiley and Sons, 1995.

[16] Long, B.C., Phipps, W.J., and Cassmeyer, V., Medical-surgical nursing: a nursing process approach. : Mosby Inc, 1993.

[17] Tyner, K.L., Exploring Chemistry in Today's World : McGraw-Hill Science, 1993.

[18] Huggett, R., Fundamentals of geomorphology : Routledge, 2007.

[19] Jacobs, B., Acids Bases and Salts : Chemistry Coach, 2004.

[20] J.R. Hook, H.E. Hall, Solid State Physics, 2nd Edition, Manchester Physics Series : John Wiley & Sons, 2010.

[21] Han, Y.S., Hadiko, G., Fuji, M., and Takahashi, M., Effect of flow rate and CO_2 content on the phase and morphology of $CaCO_3$ prepared by bubbling method. Journal of crystal growth 276,3,(2005): 541-548.

[22] Cheng, B., Lei, M., Yu, J., and Zhao, X., Preparation of monodispersed cubic calcium carbonate particles via precipitation reaction. Materials Letters 58,10,(2004): 1565-1570.

[23]   Sheng, Y., Zhou, B., Zhao, J., Tao, N., Yu, K., Tian, Y., and Wang, Z., Influence of octadecyl dihydrogen phosphate on the formation of active super-fine calcium carbonate. Journal of colloid and interface science 272,2,(2004): 326-329.

[24]   Roberts, K., Phase transitions of adsorbed carboxylic acids on zinc oxide and of zinc soaps. Infrared and X-ray diffraction investigations. Kolloid-Zeitschrift und Zeitschrift for Polymere 230,2,(1969): 357-362.

[25]   Lam, T.D., Hoang, T.V., Quang, D.T., and Kim, J.S., Effect of nanosized and surface-modified precipitated calcium carbonate on properties of $CaCO_3$/polypropylene nanocomposites. Materials Science and Engineering 501,1,(2009): 87-93.

[26]   Gao, X., Zhou, B., Guo, Y., Zhu, Y., Chen, X., Zheng, Y., Gao, W., Ma, X., and Wang, Z., Synthesis and characterization of well-dispersed polyurethane/$CaCO_3$ nanocomposites. Colloids and Surfaces A: Physicochemical and Engineering Aspects 371,1,(2010): 1-7.

[27]   Karamipour, S., Ebadi-Dehaghani, H., Ashouri, D., and Mousavian, S., Effect of nano-$CaCO_3$ on rheological and dynamic mechanical properties of polypropylene: Experiments and models. Polymer Testing 30,1,(2010): 110-117.

[28]   Gönen, M., Öztürk, S., Balköse, D., Okur, S., and Ülkü, S., Preparation and Characterization of Calcium Stearate Powders and Films Prepared by Precipitation and Langmuir- Blodgett Techniques. Industrial & Engineering Chemistry Research 49,4,(2010): 1732-1736.

[29]   Wang, C., Control the polymorphism and morphology of calcium carbonate precipitation from a calcium acetate and urea solution. Materials Letters 62,16,(2008): 2377-2380.

[30]   Gilbert, M., Sutherland, I., and Guest, A., Characterization of coated particulate fillers. Journal of materials science 35,2,(2000): 391-397.

[31] Forbes, T.Z., Radha, A.V., and Navrotsky, A., The energetics of nanophase calcite. Geochimica et Cosmochimica Acta, 75,24,(2011): 7893-7905.

[32] Liu, X., Jiang, Y., Wang, C., Li, S., Lan, X., Chen, Y., and Zhong, H., Synthesis and spectrum stability of high quality CdTe quantum dots capped with stearate groups in N-oleoylmorpholine solvent. Journal of crystal growth 312,19,(2010): 2656-2660.

[33] Wang, C., Xu, Y., Liu, Y., and Li, J., Synthesis and characterization of lamellar aragonite with hydrophobic property. Materials Science and Engineering 29,3,(2009): 843-846.

[34] Y. Sheng, B. Zhou, J.Z. Zhao, N.N. Tao, K.F. Yu, Y.M. Tian, Z.C. Wang, J., Influence of octadecyl dihydrogen phosphate on the formation of active super-fine calcium carbonate. Colloid Interface Sci 272,2,(2004): 326-329.

[35] D.K. Eeum, K.M. Kim, K. Naka, Y. Chujo, J. Mater. Chem. 12 (2002) 2449–2452.

[36] Babou-Kammoe, R., Hamoudi, S., Larachi, F., and Belkacemi, K., Synthesis of $CaCO_3$ nanoparticles by controlled precipitation of saturated carbonate and calcium nitrate aqueous solutions. The Canadian Journal of Chemical Engineering 90,1,(2012): 26-33.

[37] S. Warren, Perkins, Surfactants -A primer, dyeing, printing and finishing (1998), 51-54.

[38] Gopi, S.P., and Subramanian, V.K., Polymorphism in $CaCO_3$-Effect of temperature under the influence of EDTA (di sodium salt). Desalination 297,3,(2012): 38-47.

[39] Vucak, M., Pons, M.-N., Peric, J., and Vivier, H., Effect of precipitation conditions on the morphology of calcium carbonate: quantification of crystal shapes using image analysis. Powder technology 97,1,(1998): 1-5.

[40]   Yu, J., Lei, M., Cheng, B., and Zhao, X., Effects of PAA additive and temperature on morphology of calcium carbonate particles. Journal of Solid State Chemistry 177,3,(2004): 681-689.

[41]   Hu, Z., and Deng, Y., Synthesis of needle-like aragonite from calcium chloride and sparingly soluble magnesium carbonate. Powder technology 140,1,(2004): 10-16.

[42]   Gabrielli, C., Maurin, G., Poindessous, G., and Rosset, R., Nucleation and growth of calcium carbonate by an electrochemical scaling process. Journal of crystal growth 200,1,(1999): 236-250.

[43]   Zhou, G.-T., Yao, Q.-Z., Ni, J., and Jin, G., Formation of aragonite mesocrystals and implication for biomineralization. American Mineralogist 94,2-3,(2009): 293-302.

[44]   Wenzel, R.N., Resistance of solid surfaces to wetting by water. Industrial & Engineering Chemistry 28,8,(1936): 988-994.

[45]   Fievet, F., Fievet-Vincent, F., Lagier, J.-P., Dumont, B., and Figlarz, M., Controlled nucleation and growth of micrometre-size copper particles prepared by the polyol process. Journal of Materials Chemistry 3,6,(1993): 627-632.

[46]   Sun, B.-C., Wang, X.-M., Chen, J.-M., Chu, G.-W., Chen, J.-F., and Shao, L., Synthesis of nano-$CaCO_3$ by simultaneous absorption of CO_2 and NH_3 into $CaCl_2$ solution in a rotating packed bed. Chemical Engineering Journal 168,2,(2011): 731-736.

[47]   Wang, M., Zou, H.K., Shao, L., and Chen, J.F., Controlling factors and mechanism of preparing needlelike $CaCO_3$ under high-gravity environment. Powder technology 142,2,(2004) 166-174.

[48]   Randolph, Alan D., and Maurice A. Larson. Theory of particulate processes: analysis and techniques of continuous crystallization. Vol. 1. New York: Academic press, 1971.
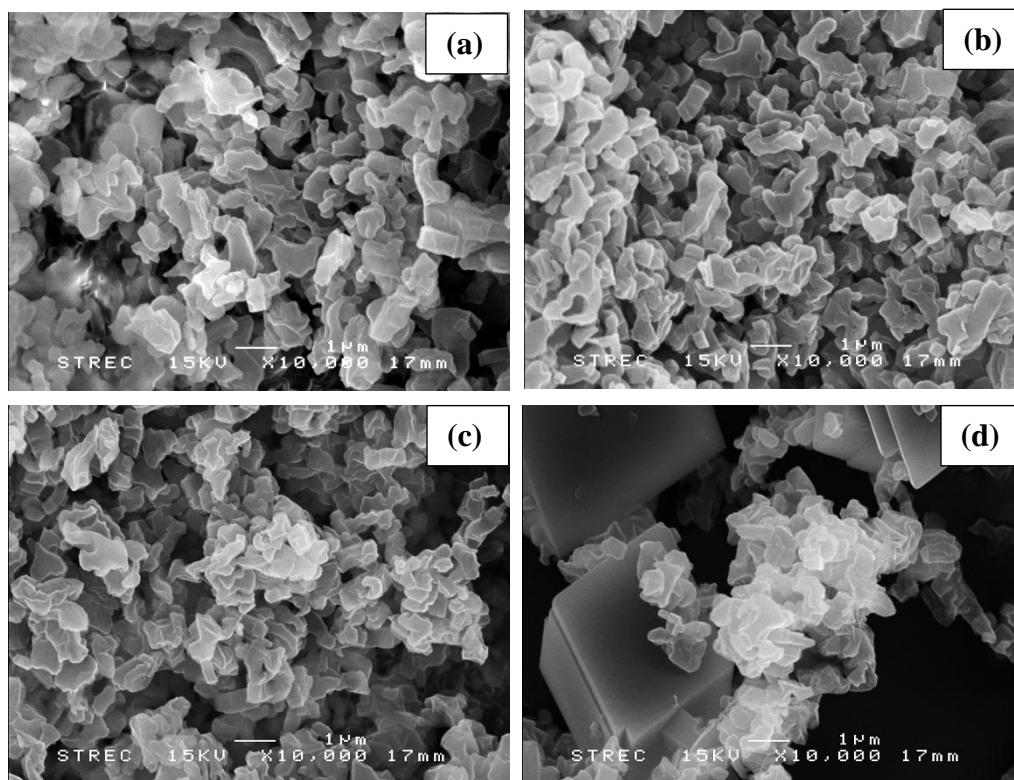
APPENDICES

APPENDIX A

SEM Image of precipitated CaCO$_3$

Figure A1 SEM images of CaCO$_3$ particles prepared at constant incubation temperature (60 °C) of (a) 1mM, (b) 2mM, (c) 3 mM and (d) 4mM
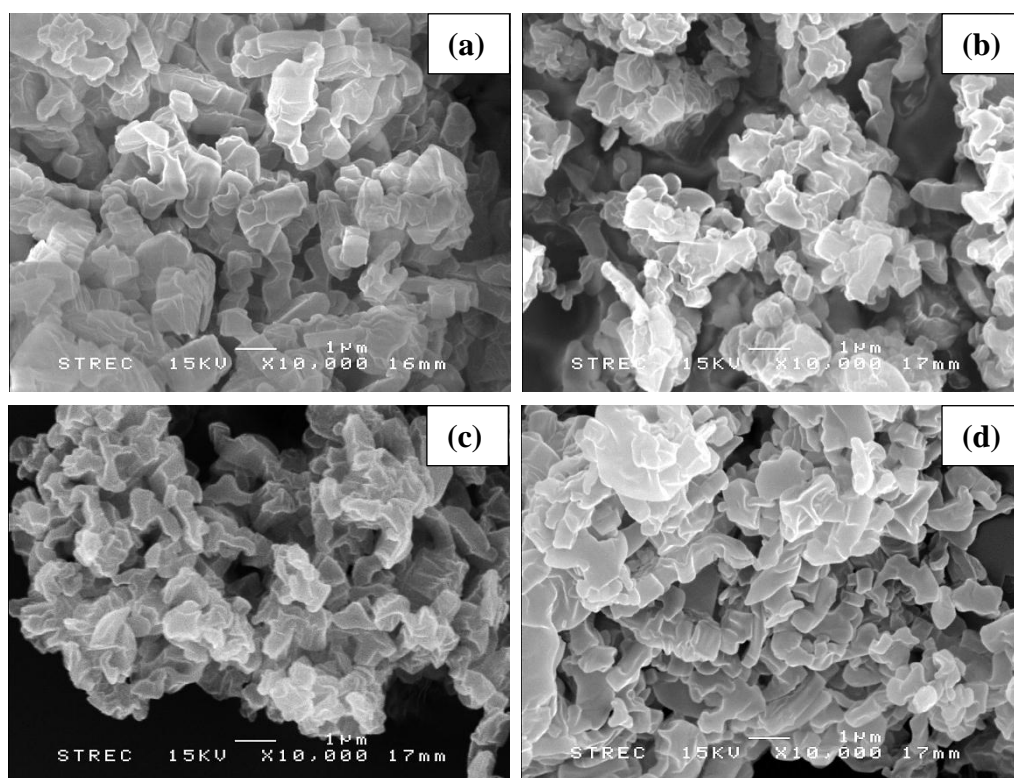
Figure A2 SEM images of CaCO$_3$ particles prepared at constant incubation temperature (90 °C) of (a) 1mM, (b) 2mM, (c) 3 mM and (d) 4mM
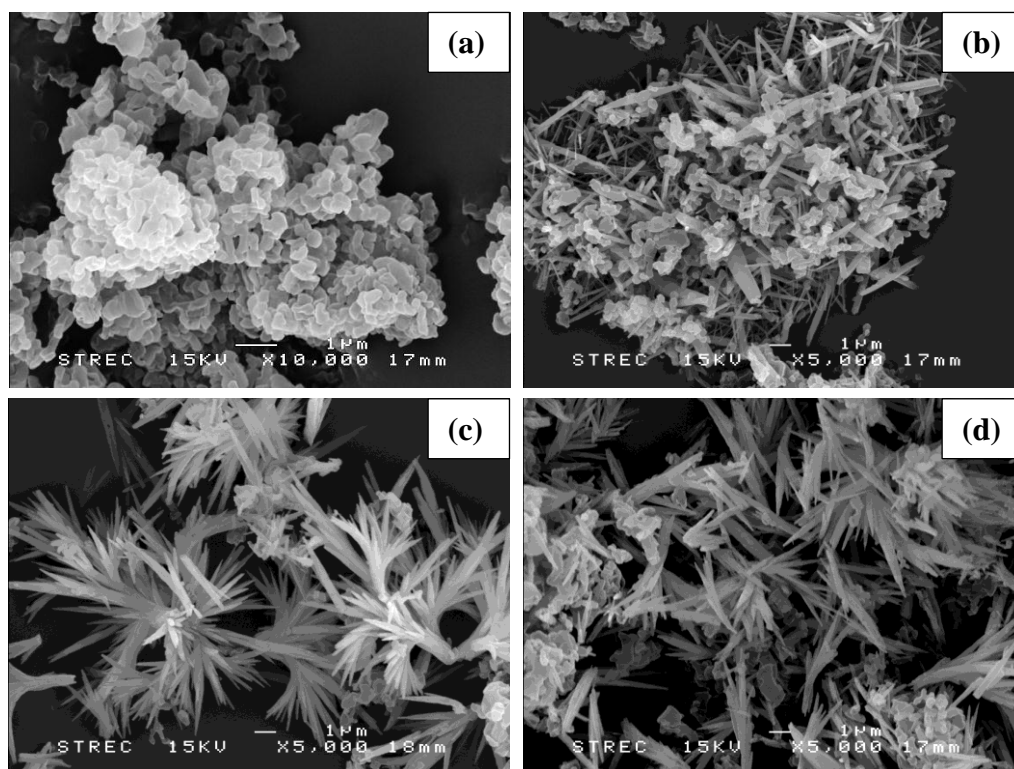
Figure A3 SEM images of CaCO$_3$ particles prepared at constant carbonation temperature (60 °C) of (a) 1mM, (b) 2mM, (c) 3 mM and (d) 4mM
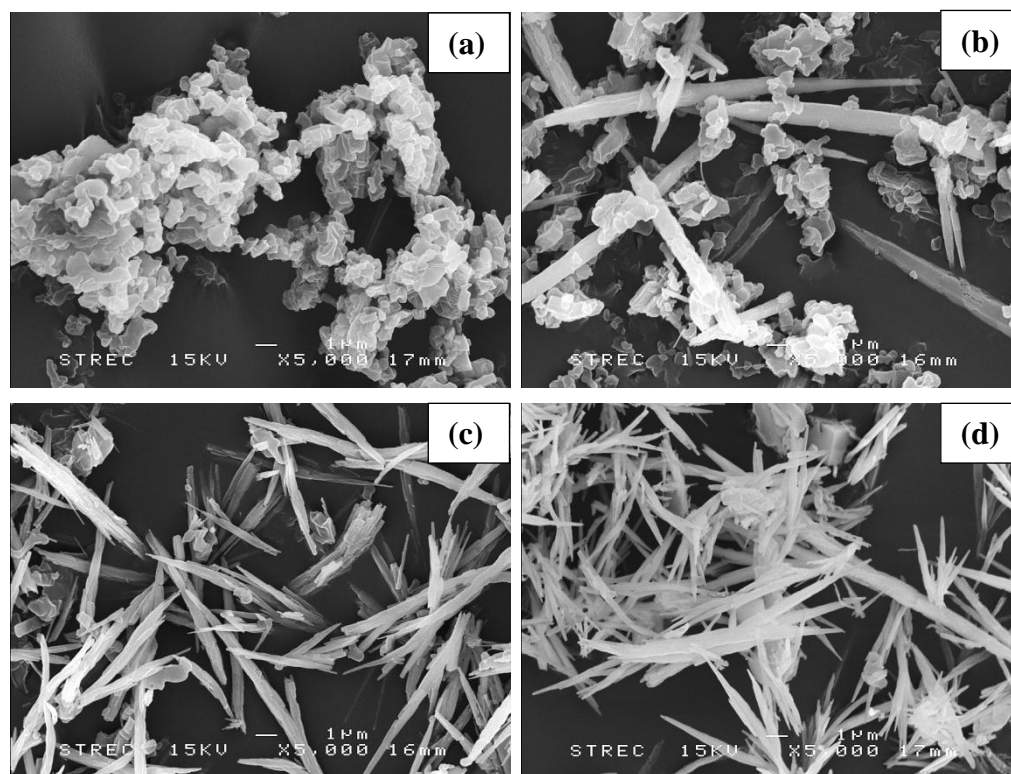
Figure A4 SEM images of CaCO$_3$ particles prepared at constant carbonation temperature (90 °C) of (a) 1mM, (b) 2mM, (c) 3 mM and (d) 4mM
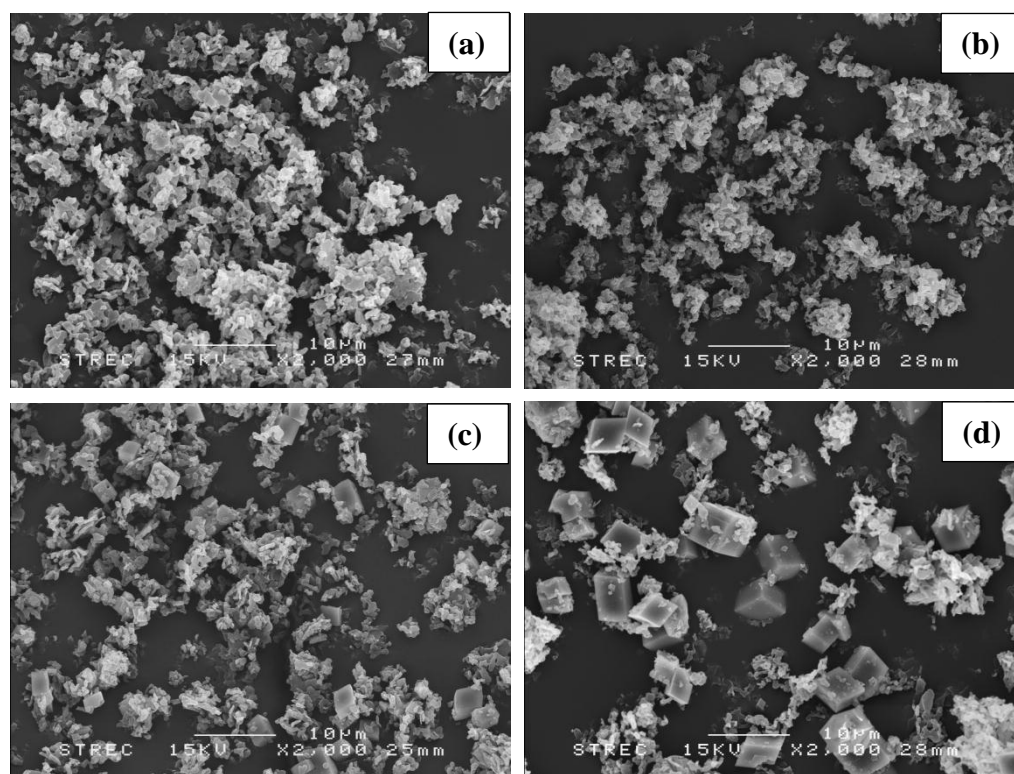
Figure A5 SEM images of CaCO$_3$ particles prepared at constant total CO$_2$/N$_2$ flow rate 0.1 L/min of (a) 1mM, (b) 2mM, (c) 3 mM and (d) 4mM
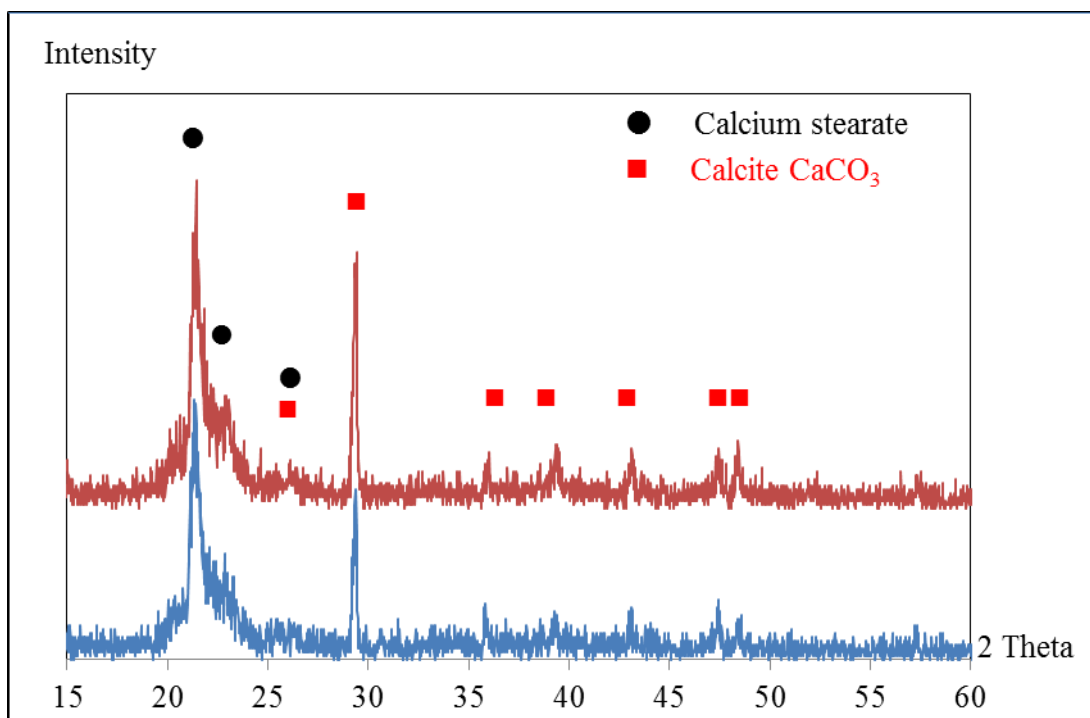
APPENDIX B

Precipitated CaCO$_3$ from Calcium stearate

Figure B1 X-ray diffraction diagrams of products prepared from calcium stearate at different initial CaCO$_3$ concentration (a) 2mM and (b) 4mM
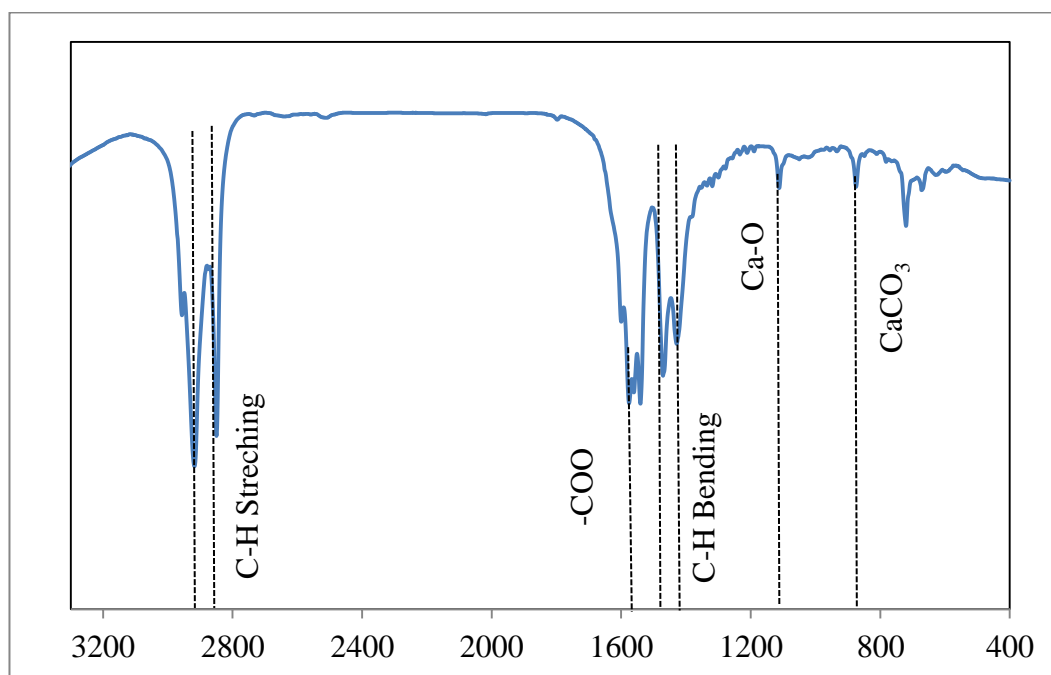
Figure B2 FTIR of products prepared from calcium stearate at 4mM initial CaCO$_3$ concentration

VITAE

Miss Supasita Yingyong was born in November 18, 1986, in Chonburi, Thailand. She completed her high-school education at Chonkanyanukoon School, in Chonburi, in 2005. She entered to Department of Chemistry, Faculty of Science, Chulalongkorn University. After graduation the Bachelor degree, in 2009, she decided continuously to study in Master degree in Center of Excellence in Particle Technology at Department of Chemical Engineering, Faculty of Engineering, Chulalongkorn University. She obtained the this degree with the thesis entitled "Synthesis of hydrophobic $CaCO_3$ nanoparticles using stearic acid as surface modifier"